Outdoor Laboratory and Testbed for Bridge Health

FINAL REPORT

Richard L. Wood (PI); Mitra Nasimi, Bowen Yang, Christine E. Wittich (co-PI); Joshua S. Steelman (co-PI); Jay A, Puckett (co-PI); Daniel G. Linzell (co-PI); Jinying Zhu (co-PI), Mohammad Ebrahim Mohammadi

University of Nebraska-Lincoln

Department of Civil and Environmental Engineering

900 N 16th St, Lincoln, NE 68588

Sponsored By

Nebraska Department of Transportation and U.S. Department of Transportation Federal Highway Administration

June 2022

NEBRASKA
Good Life. Great Journey.
DEPARTMENT OF TRANSPORTATION

UNIVERSITY OF Nebraska® Lincoln

1. Report No. M107	2. Government Accession No.	3. Recipient's Catalog No.
4. Title and Subtitle M107: Outdoor Laboratory and Testbed for Bridge Health		**5. Report Date** June 2022 **6. Performing Organization Code**
7. Author(s) Richard L. Wood, Mitra Nasimi, Bowen Yang, Christine E. Wittich, Joshua S. Steelman, Jay A. Puckett, Daniel G. Linzell, Jinying Zhu, Mohammad Ebrahim Mohammadi		**8. Performing Organization Report No.** SPR-P1(20) M104
9. Performing Organization Name and Address University of Nebraska-Lincoln 1400 R St, Lincoln, NE 68588		**10. Work Unit No.** **11. Contract** 26-1121-4048
12. Sponsoring Agency Name and Address Nebraska Department of Transportation Research Section 1500 Hwy 2 Lincoln, NE 68502		**13. Type of Report and Period Covered** Final Report July 2019 – June 2022 **14. Sponsoring Agency Code**
15. Supplementary Notes		

16. Abstract

Due to the aging problem of bridges and the limited financial resources in the United States, it is necessary to form a deeper understanding of existing, aging bridges in an effort to extend their in-service life. To address this problem, researchers from the University of Nebraska-Lincoln (UNL) and engineers from the Nebraska Department of Transportation (NDOT) identified three, out-of-service bridges (two steel and one concrete) to establish the Nebraska Outdoor Bridge Lab (NOBL). As the first step in NOBL's development, geometric surveys of the current condition of each bridge were produced using lidar and Structure-from-Motion (SfM). This data contributed to the generation of finite element analysis models for each bridge, which were used to anticipate bridge response under various loading patterns, and were validated using measured ambient vibration tests. Live load demonstrations were further performed for each bridge under various traffic loads. Geometric data, finite element models, and the results of the live load demonstrations are detailed in this report and are available for use by researchers and practitioners utilizing the NOBL facility moving forward. Additional potential uses of the NOBL facility are included along with areas for further research as concluding remarks in this report.

17. Key Words	18. Distribution Statement
bridge lab, damaged bridge, steel bridge, concrete bridge, live-load testing	No restrictions

19. Security Classification (of this report)	20. Security Classification (of this page)	21. No. of Pages	22. Price
Unclassified	Unclassified	66	

Form DOT F 1700.7 (8-72) Reproduction of completed page authorized

Table of Contents

List of Figures

List of Tables

DISCLAIMER

The contents of this report reflect the views of the authors, who are responsible for the facts and the accuracy of the information presented herein. The contents do not necessarily reflect the official views or policies neither of the Nebraska Department of Transportations nor the University of Nebraska-Lincoln. This report does not constitute a standard, specification, or regulation. Trade or manufacturers' names, which may appear in this report, are cited only because they are considered essential to the objectives of the report.

The United States (U.S.) government and the State of Nebraska do not endorse products or manufacturers. This material is based upon work supported by the Federal Highway Administration under SPR-P1(20). Any opinions, findings and conclusions, or recommendations expressed in this publication are those of the author(s) and do not necessarily reflect the views of the Federal Highway Administration."

ACKNOWLEDGEMENTS

This project was funded by the Nebraska Department of Transportation (NDOT) under project number M104 – Outdoor Laboratory and testbed for Bridge Health. The authors would like to express their gratitude to the following collaborators: researchers from SC Solutions, the University of Nevada at Reno (UNR), and the University of California, Los Angeles (UCLA). The external research collaborators were under the direction and supervision by Matt Bowers of SC Solutions.

Additionally, field support was generously provided by NDOT District 2 under the supervision of Dave Casper. Without the field support of District 2, the work performed and future activities could not occur at the NOBL facilities. Field support at the NOBL North Facility was also supported by the NDOT Snooper team with Seth Brashears, Mike Mosiman, and Dallas Pears. Moreover, the research team would also like to appreciate the support and assistance of the Technical Advisory Committee (TAC) throughout this project. This includes the following member (in alphabetical order): Mark Ahlman, Mark Fischer, Lieska Halsey, David Hansen, Kirk Harvey, Fouad Jaber, Kent Miller, Babrak Niazi, Tom Renninger, Mark Traynowicz, Tim Weander, Brandon Varilek, and Mike Vigil.

ABSTRACT

Due to the aging problem of bridges and the limited financial resources in the United States, it is necessary to form a deeper understanding of existing, aging bridges in an effort to extend their in-service life. To address this problem, researchers from the University of Nebraska-Lincoln (UNL) and engineers from the Nebraska Department of Transportation (NDOT) identified three, out-of-service bridges (two steel and one concrete) to establish the Nebraska Outdoor Bridge Lab (NOBL). As the first step in NOBL's development, geometric surveys of the current condition of each bridge were produced using lidar and Structure-from-Motion (SfM). This data contributed to the generation of finite element analysis models for each bridge, which were used to anticipate bridge response under various loading patterns, and were validated using measured ambient vibration tests. Live load demonstrations were further performed for each bridge under various traffic loads. Geometric data, finite element models, and the results of the live load demonstrations are detailed in this report and are available for use by researchers and practitioners utilizing the NOBL facility moving forward. Additional potential uses of the NOBL facility are included along with areas for further research as concluding remarks in this report.

1 Introduction

1.1 Project overview

The purpose of this project is to establish the Nebraska Outdoor Bridge Lab (NOBL). To accomplish this project, two steel bridges near Yutan and one concrete bridge near Omaha were selected. This project was performed in four main phases or tasks and is described herein. Before starting any site characterization or fieldwork and to increase safety, an operational and safety document was developed, and then site access was limited with additional fencing (at Yutan). Then, site characterization was done by remote sensing using point clouds generated by lidar scanning and supplemental Structure-from-Motion data using an uncrewed (or unmanned) aerial system (UAS). This site characterization provides current geometric information at each bridge site at the centimeter level, which is needed to construct the finite element analysis (FEA) models. In addition to geometric information, system identification provided a quantification of the vibrational response of the bridges under ambient vibrations to verify and calibrate the FEA models. These calibrated or refined models are updated to reflect field measurements and bridge response. These models aim to include realistic conditions of each bridge site, which may include: deterioration, boundary conditions, unintended composite action, and construction tolerances. Lastly, demonstrative live load testing was done at each bridge site to quantify and measure the bridge response under a series of live load patterns. The live load consisted of two 50-kip triaxial trucks operated at various speeds, spacings, and configurations.

1.2 Benefits and tasks

The project aims to establish a research and educational facility related to bridge health and the training of students/future engineers, bridge engineers, and bridge inspectors. Due to the closed-traffic conditions of these bridges, this laboratory facility enables a test bridge to explore analytical modeling (with calibration), remote sensing, diagnostic techniques, and structural health monitoring. This project will provide a detailed

characterization of realistically aged bridges (two steel bridges at Yutan and one concrete bridge at Omaha). In the long term, this project aims to study key questions on bridge health to address statewide and national needs.

This project has four identified research tasks to achieve and meet the project objectives. An overview flowchart is shown in Figure *1.1* which outlines the interconnectedness and flow of the project. The four tasks include (1) Site Staging, (2) Site Characterization, (3) Facility Demonstration, and (4) Reporting. Each of these four tasks contributes to the overarching objective: *to transform three bridges into a national research and educational facility for bridge health and testing*.

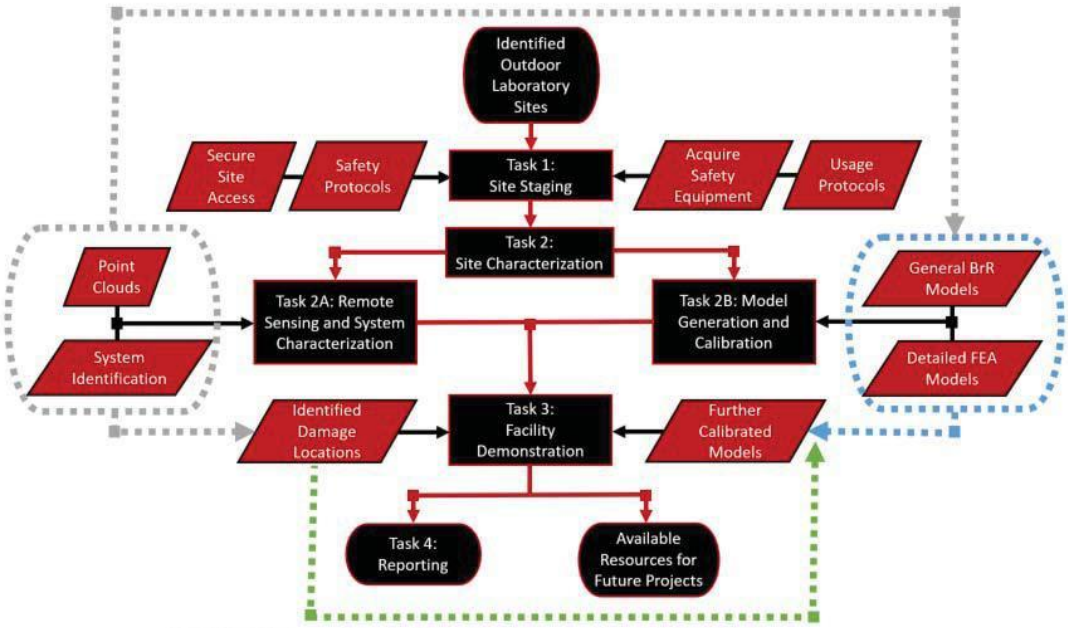

Figure 1.1. Flow chart of the research tasks.

1.3 Outline of report

This report consists of six chapters. Chapter 1 outlines the motivation for the work, defines the project, and summarizes the scope. Chapter 2 outlines the safety and operational document as well as site staging (Task 1). Chapter 3 briefly describes the three-dimensional geometric data collection for site characterization as well as the ground-penetrating radar (GPR) for assessment of the bridge deck (Task 2A). Chapter 3 also

summarizes the finite element analysis (FEA) models of the bridge site (Task 2B). Chapter 4 summarizes the demonstration with the live loads (Task 3), which includes an overview of the experiment, sensors used, processing, and quantification of the data. Chapter 5 focuses on a strain gauge assessment of the concrete bridge at Omaha (Task 3). Chapter 5 provides conclusions of this project and recommends future research topics (Task 4). Appendix A presents the Safety Protocol and Information document, as specified developed and related to the NOBL facility. Appendix B outlines and summarizes the site demonstration data (Task 3).

2 Site setup and facility establishment

2.1 Site selection

The Nebraska Outdoor Bridge Lab (NOBL) is comprised of three bridges at two sites. Currently, the bridge sites are minimally not in regular service or completely out of service. This chapter aims to describe and outline the bridge details by each site as well as the safety and operational procedures and securement of the site. This chapter closely relates to Task 1 of the project.

2.1.1 NOBL (Steel Bridges at Yutan)

The (primary) NOBL site is located on Nebraska State Route 92 over the Platte River just east of Yutan, as shown in Figure *2.1*. Herein, this is known as the "Yutan (steel) bridge site". At this site, two steel girder bridges cross the river in two separate crossings (with an island). These bridges were decommissioned in 2005 when replacement bridges were constructed just to the north of the bridge lab.

These bridges have nominal lengths of 400-feet (east bridge) and 1000-feet (west bridge). Overview photos of the bridges are illustrated in Figure *2.2*. As illustrated in Figure 2.3, these steel bridges exhibit various damage mechanisms due to environmental and mechanical loads. This includes steel girder corrosion, abutment cracking, anticipated concrete delamination, and cracking in the asphalt overlay. The east bridge consists of (4) 100-feet spans comprised of approximately 54-inch welded plate girders with pin and hanger connections. The west bridge consists of eight 112-feet spans comprised of approximately 54-inch welded plate girders with pin and hanger connections. Both bridges at this site were designed in 1960. Information, structure numbers, and properties for both steel bridges at Yutan are summarized in Table 2.1.

(a) Detailed view of NOBL lab at Yutan

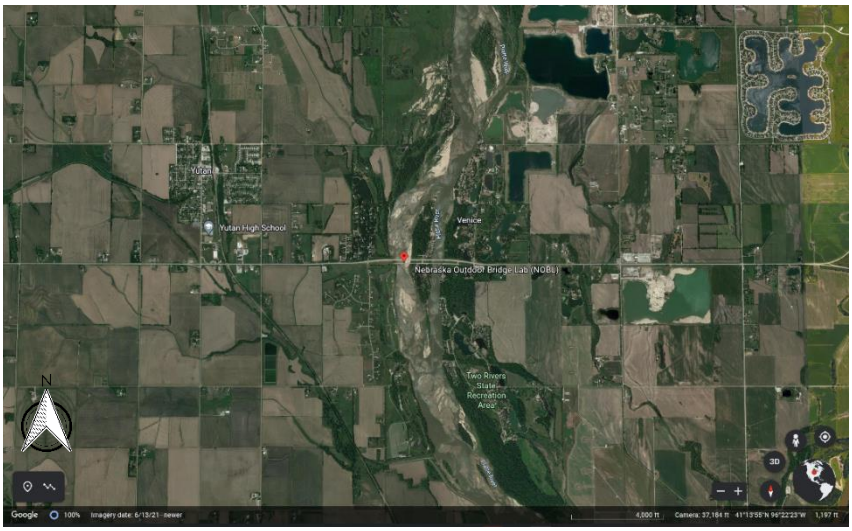

(b) Satellite view of NOBL lab at Yutan

Figure 2.1. Site view of NOBL lab at Yutan.

(a) NOBL East bridge at Yutan overview (NOBL East)

(b)Yutan west steel bridge overview (NOBL West)

Figure 2.2. Yutan Steel bridge.


(a) Example corrosion and delamination


(b) Abutment damage


(c) Pin lost at pin-hanger connection (d) bridge deck with cracking

Figure 2.3. Example images of the steel girder bridge damages at Yutan bridge site.

Table 2.1. Tabular summary of the NOBL bridges.

Description	Yutan Steel Bridge Site (East)	Yutan Steel Bridge Site (West)	Omaha Concrete Bridge
Structure Number	S092 46282R	S092 46256R	S036 02040L
Year Built	1960	1960	1979
Year Decommissioned	2005	2005	--
Bridge Length (ft [m])	600 [182.9]	1000 [304.8]	156 [47.55]
Bridge Width (ft [m])	32 [9.8]	32 [9.8]	39.5 [12]
Number of Spans	4	8	3
Span Length (ft [m])	100 [30.5]	112 [34.1]	60 [18.29]
End Span Length (ft [m]), if different	--	--	48 [14.63]
Number of Girders	4	4	5
Girder Type	Welded plate with pin and hanger connection	Welded plate with pin and hanger connection	AASHTO type 3A
Bridge Location (latitude, longitude)	State Route 92, East of Yutan, NE	State Route 92, East of Yutan, NE	State Route 36, North of Omaha, NE
Deck Surface Type	Concrete	Concrete	Concrete
Membrane	No	No	Yes
Overlay	Latex modified structural concrete	Latex modified structural concrete	Asphalt concrete (A.C)
Deck Protection	Asphalt	Asphalt	Asphalt
Deck Thickness (in [cm])	7 [17.78]	7 [17.78]	7.5 [19.05]

2.1.2 NOBL North (Concrete Bridge at Omaha)

The (other) bridge site is located on State Route 36 over the Glenn Cunningham Reservoir just north of Omaha, as shown in Figure *2.4*. Herein this is known as the “Omaha (concrete) bridge site” or “NOBL

North". This concrete bridge was originally designed for a potential four-lane divided highway expansion in 1979, but has seen only minimal traffic loads. This bridge site does experience occasional traffic associated with recreational users (e.g., horseback vehicles), training exercises (e.g., NDOT, Omaha Police Department, etc.), and construction traffic (as in 2022). The concrete bridge at Omaha consists of three spans (as shown in Figure *2.5*) of 48, 60, and 48-feet, respectively; and is comprised of AASHTO girder type 3A (Shown in Figure *2.6*). This bridge was designed in 1979 as a pair, at the time of construction, this bridge was one of the twenty bridges that received an asphalt with waterproofing membrane on the original construction and before opening to service. Now the north pair of the bridge is unused while the south pair of the bridge has supported regular traffic of Nebraska State Highway 36 since construction. As illustrated in Figure *2.7*, various damage modes can be observed in this structure despite its minimal use of mechanical loads (vehicles) as well as environmental loads. This includes localized scour at the abutment, abutment cracking, suspected delamination near the bridge deck weep holes, and cracks in the asphalt deck overlay. Information, structure number, and properties for this bridge are summarized in Table 2.1

.

(a) Detailed view of NOBL North bridge in Omaha

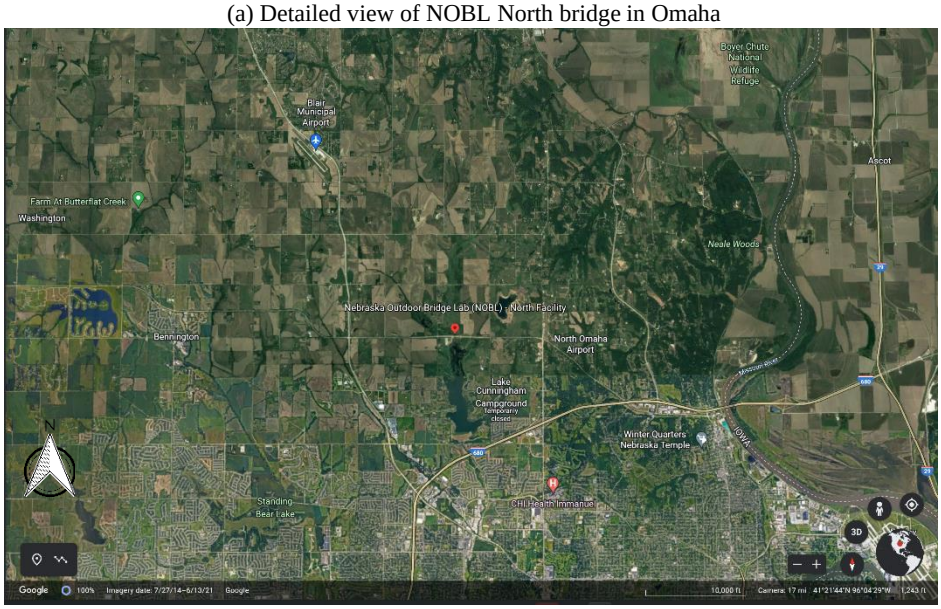

(b) Satellite view of NOBL lab located in North Omaha

Figure 2.4. Site view of NOBL North bridge in Omaha .

Figure 2.5. Overview of the NOBL North bridge in Omaha .

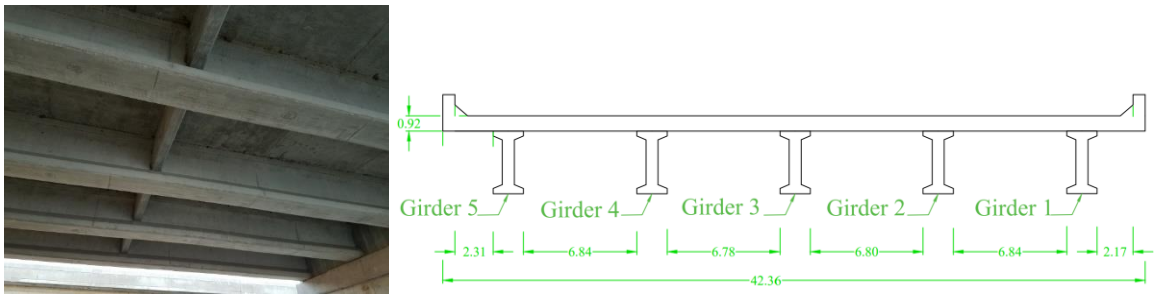

(b) View of concrete girders from below (b) cross-section of the concrete bridge

Figure 2.6. Cross-section and girder details related to NOBL North bridge in Omaha .

(a) Abutment Damage

(b) Bridge deck condition with cracks

(c) Delamination at weep hole

(d) East abutment damage and exposed pile

Figure 2.7. Damage example images of the NOBL North bridge in Omaha site.

2.2 Safety and operational document

These bridges were previously selected for educational, research, and outreach/engagement purposes by both UNL and NDOT in joint collaboration. To facilitate operation and safety at these sites, a dedicated operations document was generated and reviewed by the UNL Office of Environmental Safety. The document in its entirety is compiled in Appendix A (Safety and Operational Document) as well as hosted on the NOBL website (http://nobl.unl.edu). Note this document aims to be updated regularly, given

anticipated personnel and operational changes at UNL. The latest version of this document is compiled in this report.

2.3 Site staging and security

At Yutan, these bridges are in close proximity to routine traffic loads (Nebraska State Route 92) as well as see occasional and unapproved recreational uses, despite both of these two bridges at Yutan posted for no trespassing. Fencing gates are installed at this site for safety and limit access for personnel and equipment uses at this site, as part of this project. The purpose of these gates is to create a safe laboratory environment for both the UNL/NDOT participants, their invited guests, and the public as well as permit access by approved personnel. To accomplish this, fencing was installed to limit access to the general public and traffic. Access to open these gates is controlled by a state-owned padlock (with a key for DOT and other state agencies' access (e.g., Nebraska State Patrol)) and a numeric combination lock (for NOBL uses). Figure 2.8 shows the location and details of each of the abutments of the NOBL facility at Yutan. The official signature for the facility exists on both Yutan bridges. Moreover, no fencing or gates were placed at the NOBL North site in Omaha.

2.4 Intermediate conclusions

Task 1 of this project, as summarized in this chapter, enabled safe and controlled usage of the bridge facilities for various interested parties and project participants. This was done in close coordination with NDOT for safety and right-of-way (ROW) permits. The safety document for site access is maintained for all interested parties to review before facility usage. With the site secured, additional tasks were then able to be completed.

(a) Gate locations in NOBL lab at Yutan

(b) Gate C detailed view

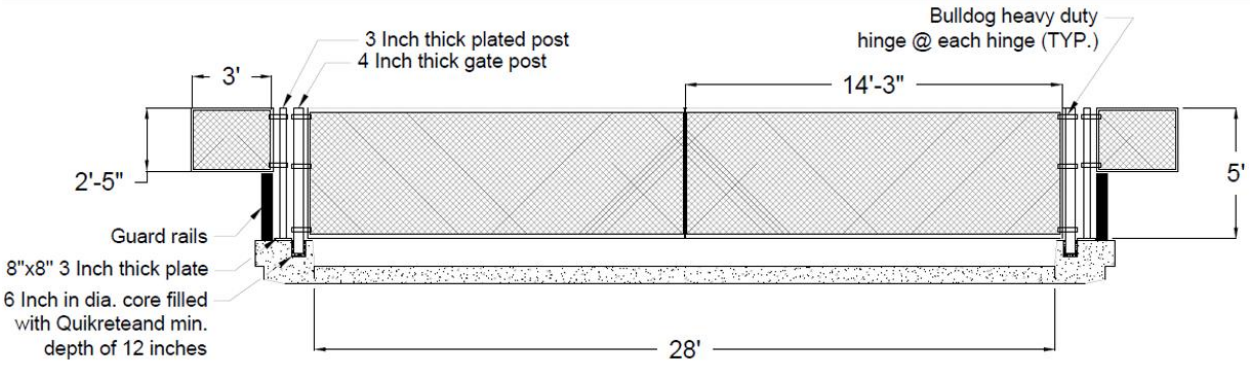

(c) Geometric information of gates

Figure 2.8. Detailed information of the gates placed in NOBL lab at Yutan.

3 Initial site characterization

3.1 Introduction

The three bridge structures at Yutan and Omaha have experienced a variety of environmental and service loads since their initial construction. Given construction tolerances and changing bridge conditions, one of the earliest tasks was to nondestructively characterize these bridges in terms of structural and geometric properties for further investigations. This was accomplished using lidar and Uncrewed (or unmanned) Aerial Systems (UAS) surveying for the geometry, initial accelerometer measurements for system identification, preliminary finite element analysis (FEA) model construction, and ground-penetrating radar scanning. Summary details are provided below. This chapter closely relates to Task 2 of the project.

3.2 Lidar and UAS

Light detection and ranging (lidar) scans were collected using two scanners, Faro Focus^{3D} X130 and S350 laser scanners, for each bridge structure. The Faro Focus^{3D} X130 lidar or laser scanner and Faro focus S350 laser scanner was utilized during the site investigations and are used to scan profiles in distance ranging up to 130 (426 [ft]) and 350 (1148 [ft]) meters, respectively. For terrestrial-based scanning, multiple scans at various locations with adequate overlap are required to create a dense point cloud, reduce areas of occlusions, and improve the alignment accuracy. These points aid in quantifying the static geometry of the bridges. One delay during the project did arise in the field deployment of the S350 lidar scanner. This sustained damage in the field at the NOBL North site given traffic-induced wind but was successfully repaired after an unfortunate and extended delay.

The lidar scan files are uploaded into various computer software platforms, such as Faro Scene, Cloudcompare, and Autodesk Recap, for point cloud processing for take-off geometry. Each individual scan file contains inherent noise, which is unavoidable. Most of these points are removed with segmentation (manually) and filtering techniques. A statistical outlier removal (SOR) filter is used to eliminate most of

the noise and erroneous points with automation, especially those caused by sharp object edges. This filter estimates the mean distance between the inputted number of random points and removes the points outside of the specified standard deviation threshold. Filtered point clouds provide accurate information about the geometric information and could use for further comparison purposes as the bridge condition changes.

Uncrewed (or Unmanned) Aerial Systems (UASs or commonly known as drones) are one of the commonly used methods for mapping. In this research, a DJI Inspire 2 UAS was used along with ground control points using a Global Navigation Satellite System (GNSS) survey technique georeference the collected data. Georeferencing was implemented through the use of ground control points (GCPs) and checkpoints (CPs). The use of GCPs significantly increases the accuracy of the obtained data in PIX4Dmapper software and this was achieved at the centimeter level horizontally 5 cm (2 in), as confirmed in the checkpoints. However, the accuracy of the collected data depends on the vegetation, overlap of the images, the precision of the real-time kinematic (RTK) survey, and light condition (on the images). The maximum error was below 8 cm (3 in) in the vertical direction. In the final step (for each bridge site), the two point clouds as generated using UAS and lidar scanner were uploaded to CloudCompare software and aligned with each other by selecting at least three common points using a technique called Single Value Decomposition (Liao et al., 2020) The point clouds can then be used to quantify areas of spalling or corrosion, measure deflection, and generate the necessary geometry for finite element analysis (FEA) modeling. In this project, the primary usage of the point clouds was for geometric input for the FEA modeling as well as general visualization of the sites. Figure 3.1 shows the final point cloud generated for the three selected bridges. Note visualizations of these sites are also available on the NOBL website (NOBL, n.d.).

(a) NOBL East steel bridge at Yutan (NOBL East)

(b) NOBL West steel bridge at Yutan (NOBL West)

(c) NOBL North concrete bridge in Omaha (NOBL North)

Figure 3.1. Point clouds for the three selected bridge sites.

3.3 Finite element analysis (FEA) models

To identify the response of the bridge under various loads, a numerical finite element analysis (FEA) model analysis was performed using the point cloud data geometry and bridge plans to obtain the modal frequencies and other response behavior. The FEA modeling of the bridge was generated using CSiBridge to study the bridge response, where these models are available for use by interested parties. These bridge models were developed based on the material properties identified in the available reference (Ocel, 2021), plan drawings, and engineering judgment. For the deck concrete compressive strength, while it is expected that an undamaged concrete deck strength would exceed the 28-day design compressive strength of 3.0 ksi, no overstrength is considered in these models. By neglecting the overstrength here, this accounts for some concrete degradation in the deck which is exhibited in the photos and field visit. This assumption results in a lower deck stiffness due to existing deck deterioration and it will be assessed in the field for its validity. Table *3.1* shows the material properties used for modeling. Figure *3.2* shows the developed finite element model of the bridges.

Table 3.1. Material properties used to model NOBL bridges.

Properties	Yutan Steel Bridge Site	Omaha Concrete Bridge
Deck concrete strength ([ksi])	3.0	3.0
Concrete elastic modulus ([ksi])	3604.9	3604.9
Reinforcement steel	Gr60	Gr60
Girder steel	A7	
Web height ([inches])	54	--
Web thickness ([inches])	1	--
Flange width ([inches])	13.8	--
Flange thickness ([inches])	1.79	--
Girder concrete strength ([ksi])	--	4
Prestress tendon	--	GR270
Girder	--	AASHTO- Type 3A

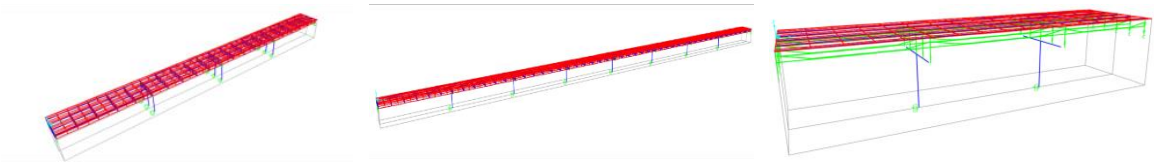

(a) NOBL East bridge at Yutan (b) NOBL West bridge at Yutan (c) NOBL North bridge in Omaha

Figure 3.2. CSiBridge finite element modeling of the three selected bridges.

An eigenvalue analysis was also conducted for each of these models. Table *3.2* summarizes the three natural frequencies obtained from the initial numerical model analysis. Based on the achieved natural frequencies NOBL concrete bridge at North Omaha (NOBL North) is more rigid than the East Yutan bridge. Moreover, the East Yutan bridge (NOBL East) is less flexible than the West bridge (NOBL West). This behavior is anticipated, as in general, when various parameters are consistent, a steel bridge is often more flexible than concrete and the flexibility of a bridge increases with length (Martindale et al., 2019; and etc.). Figure *3.3*

shows the mode shapes generated for each selected bridge in CSiBridge. System identification was done based on the first three natural frequencies using the Artemis platform (Döhler et al., 2017). As noted in a previous NDOT project on Inverted Tees Bridges, the extended unweighted principal component method provided clear results (Martindale et al., 2019). Note the dynamic properties of these initial models have been verified/confirmed in Chapter 4.

Table 3.2. Natural frequency for the three selected bridges from the FEA models.

Mode	NOBL East Frequency (Hz)	NOBL West Frequency (Hz)	NOBL North Frequency (Hz)
1	3.45	2.77	9.29
2	4.17	3.02	9.78
3	4.31	3.15	11.02

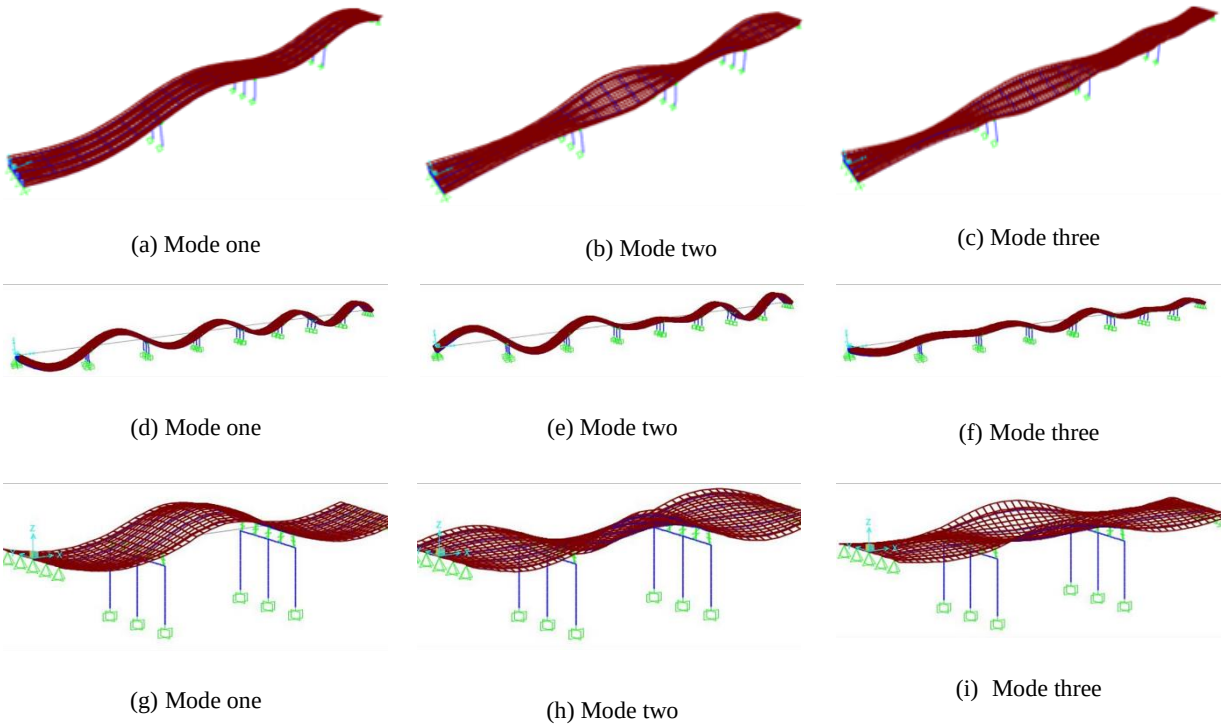

(a) Mode one (b) Mode two (c) Mode three

(d) Mode one (e) Mode two (f) Mode three

(g) Mode one (h) Mode two (i) Mode three

Figure 3.3. Mode shapes of the three selected bridges; (a), (b), (c) NOBL East steel bridge at Yutan; (d), (e), (f) NOBL West steel bridge at Yutan; (g), (h), (i) NOBL North concrete bridge in Omaha.

3.4 GPR scanning

Ground Penetrating Radar (GPR) scanning is a signal-based non-destructive technique that is widely used to detect surface objects. In this research, GPR has been used to determine rebar and the potential location of the concrete deterioration. GPR transmits radar pulses and based on the obtained reflections from rebars, and wave velocity, the depth of the rebar can be calculated. At the same time, the amplitude of the reflected waves was measured along the span of the bridge. Lower amplitude and weaker signal show the potential location of the deck cover concrete deterioration or rebar corrosion (Zhu & Pashoutani, 2020). In this project, the lower amplitude signals likely represent significant concrete degradation and/or delamination. Figure *3.4* shows GPR mapping for three selected bridges. The NOBL East bridge structure at Yutan demonstrates significantly degraded concrete at the approach spans as well as distributed throughout. To validate the results obtained from the GPR scanning, in the future work it would be desirable to do select coring in arbitrary locations of the bridge decks. However, these locations have not been finalized.

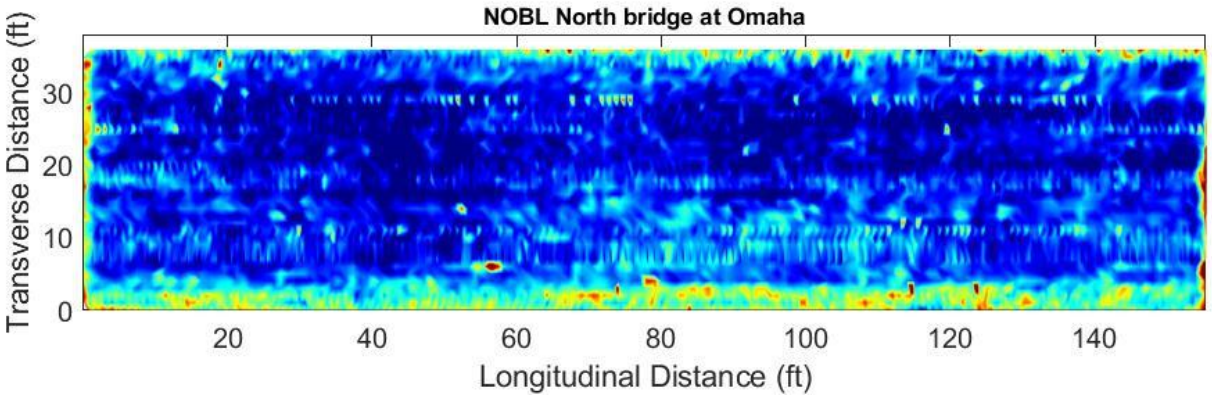

(a) NOBL North bridge at Omaha

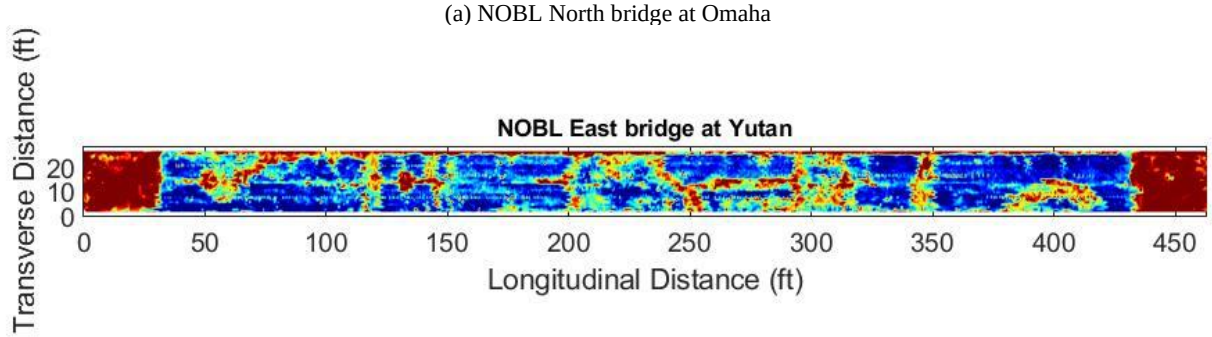

(b) NOBL East bridge at Yutan

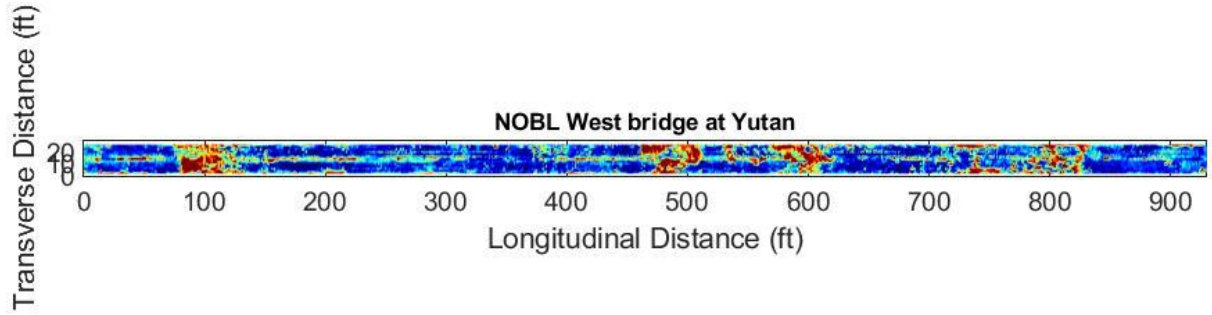

(c) NOBL West bridge at Yutan

Figure 3.4. Concrete deck GPR scan mapping results in the entire bridge width and length.

3.5 Intermediate conclusions

Task 2 of this project, as summarized in this chapter, provides the site characterization data for each of the bridge sites. This initial site characterization data consists of high-detailed, high-fidelity point clouds, finite element analysis models, and ground-penetration radar scans of each bridge site. This data is available for use by request. It is also envisioned that this data will support the project's goal of establishing a research and educational facility related to bridge health and the training of students/future engineers, bridge engineers, and bridge inspectors.

4 Site demonstration

4.1 Overview

The purpose of this chapter is to demonstrate how the NOBL facilities can be used by other researchers, engineers, students, etc. In this task, the focus was on the evaluation and assessment of bridge health (of the three bridges) using non-destructive testing techniques. To help identify dynamic responses, a series of accelerometers and strain gauges are mounted to the deck and girders of the bridges to collect vibrational response data during the live loads. These sensors were explicitly used by the UNL research team. Live loads were supplied to the bridges using a set of two triaxial trucks of 50-ton capacity (nominal weight).

Within this research, the primary measurement of the dynamic behavior was uniaxial piezoelectric accelerometers. This type of sensor has been shown viable for civil infrastructure (bridges and buildings) on various frequencies with notable results (Bose, et al., 2015) and (Martindale, et al., 2019). This sensor measures the vibrations of the bridge, which vary on truck speed, the weight of the truck, type of the bridge structure, condition of the deck, and sensor location or placement. To generalize the sensor response from the time domain, peak acceleration envelope values are summarized for each of the live loading cases (per bridge site). The objective of this task and chapter is to quantify the bridge response under various traffic loads to inform this project (in terms of modeling) as well as future research. This chapter closely relates to Task 3 of the project.

4.2 Sensor overview

Datasets from the bridge were collected using different types of sensors such as wired and wireless accelerometers, strain gauges, video monitoring, and displacement gauges. This was done for each pass of the live load (one or two triaxial trucks at various speeds, patterns, etc.). Note this chapter focuses exclusively on the uniaxial accelerometers, where Chapter 5 discusses the strain gages as deployed on NOBL North. Moreover, external researchers used wireless accelerometers, video monitoring, and

displacement gages in support of their FHWA SBIR Project (SC Solutions, n.d.). The upcoming section will provide a summary of the wired accelerometers.

4.2.1 Uniaxial accelerometers

To collect data during the field experiments a series of cabled uniaxial sensors were used to record the bridge vibration response of the bridge system under various load patterns. The uniaxial sensors are wired piezoelectric accelerometers, shown in Figure *4.1*. The PCB 393B04 accelerometers have a measurement range of ±5g and a broadband resolution of 3x10 µg root mean square (RMS). This type of sensor is a high-sensitivity seismic accelerometer that is extremely sensitive to indiscernible vibrations. It has been successfully used on bridge structures in the past, but is heavily used and validated in the NDOT Inverted Tee Project (Martindale, et al., 2019). This sensor collected data at a sampling frequency of 2096 Hz, which provided ample frequency resolution for post-processing to quantify the bridge response reliably.

Figure 4.1. Example placement of a wired uniaxial accelerometer.

4.3 Deck setup

During the field experiments, accelerometers are attached to the top portion of the deck of the bridge in each span at 1/3 points along the length. Figure *4.2* shows example instrumentation for NOBL North bridge. For this type of setup, accelerometers are typically placed in opposing pairs on the deck curb (north and south curbs on the deck). The deck setup for NOBL North is shown in Figure *4.3*. An assembly of the

NOBL East and NOBL West plots is compiled in Appendix B. Note that the sensor placements at NOBL East and NOBL West (at the Yutan site) closely mimic the placements at NOBL North. Due to the number of spans at NOBL West, only the east half of the bridge was instrumented by the UNL team. An upcoming and collaborative dataset for the entire bridge is still being processed by the external researchers (in collaboration with the UNL team) under the direction of SC Solutions.

(a) deck setup

(b)) girder setup for NOBL North bridge

Figure 4.2. Field accelerometer instrumentations as placed for NOBL North.

4.4 Girder setup

This accelerometer setup quantifies the response of each girder under the live load and is indicative of the potential independent girder response (due to insufficient transverse load distribution). This type of accelerometer placement was done on a single span on each bridge structure. The NOBL East girder setup was performed on only four girders of the first span of the bridge from the east side. In NOBL West accelerometer was mounted to the four girders from the east and middle span of the bridge. For the NOBL North accelerometers were installed only to five girders of the first span from the east. The number of girders available for sensor placements was a function of the available equipment and site conditions. The girder setup for NOBL North bridge is shown in Figure *4.3,* and Figure *4.4*. Note that the sensor placements on the bottom side of the girders at NOBL East and NOBL West (at the Yutan site) closely mimic the placements at NOBL North.

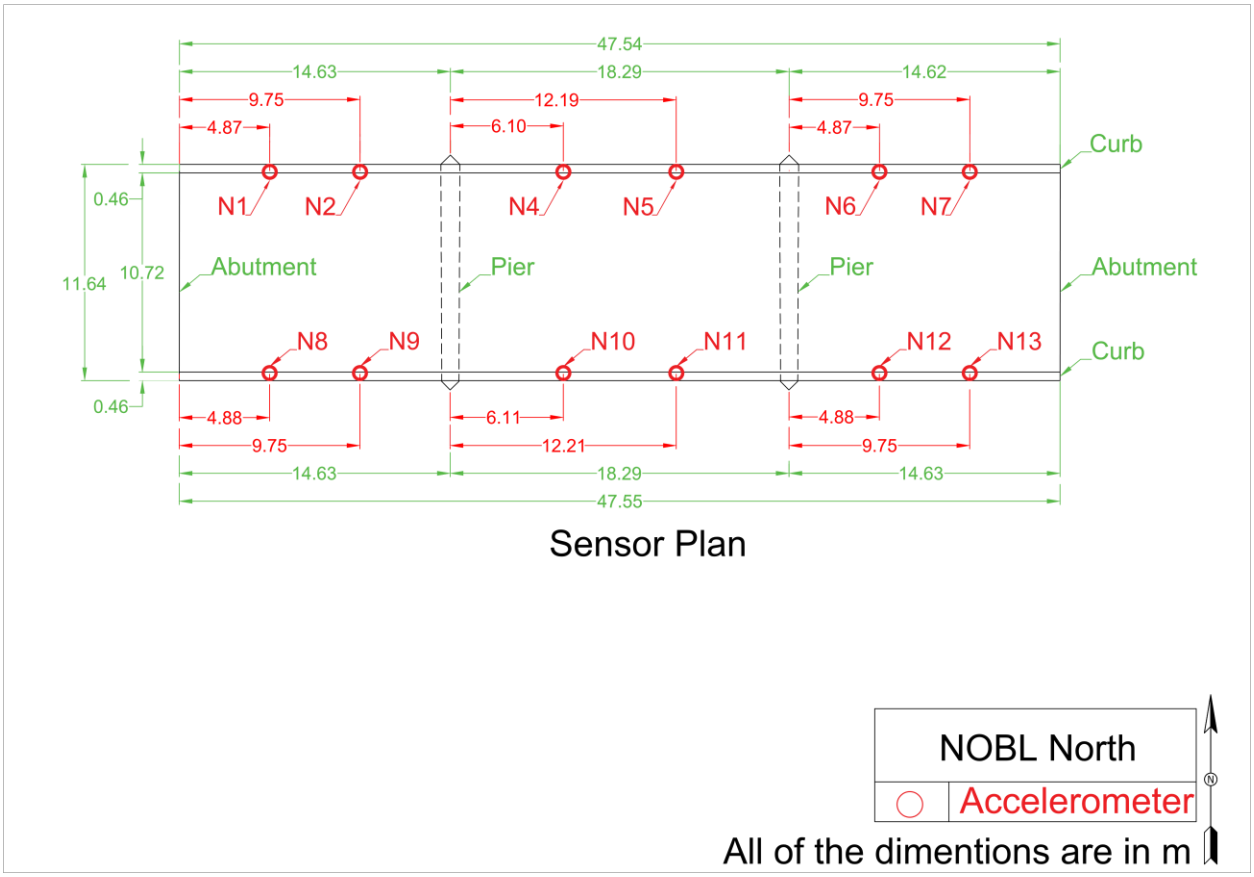

Figure 4.3. Locations of the accelerometer instrumented for NOBL North.

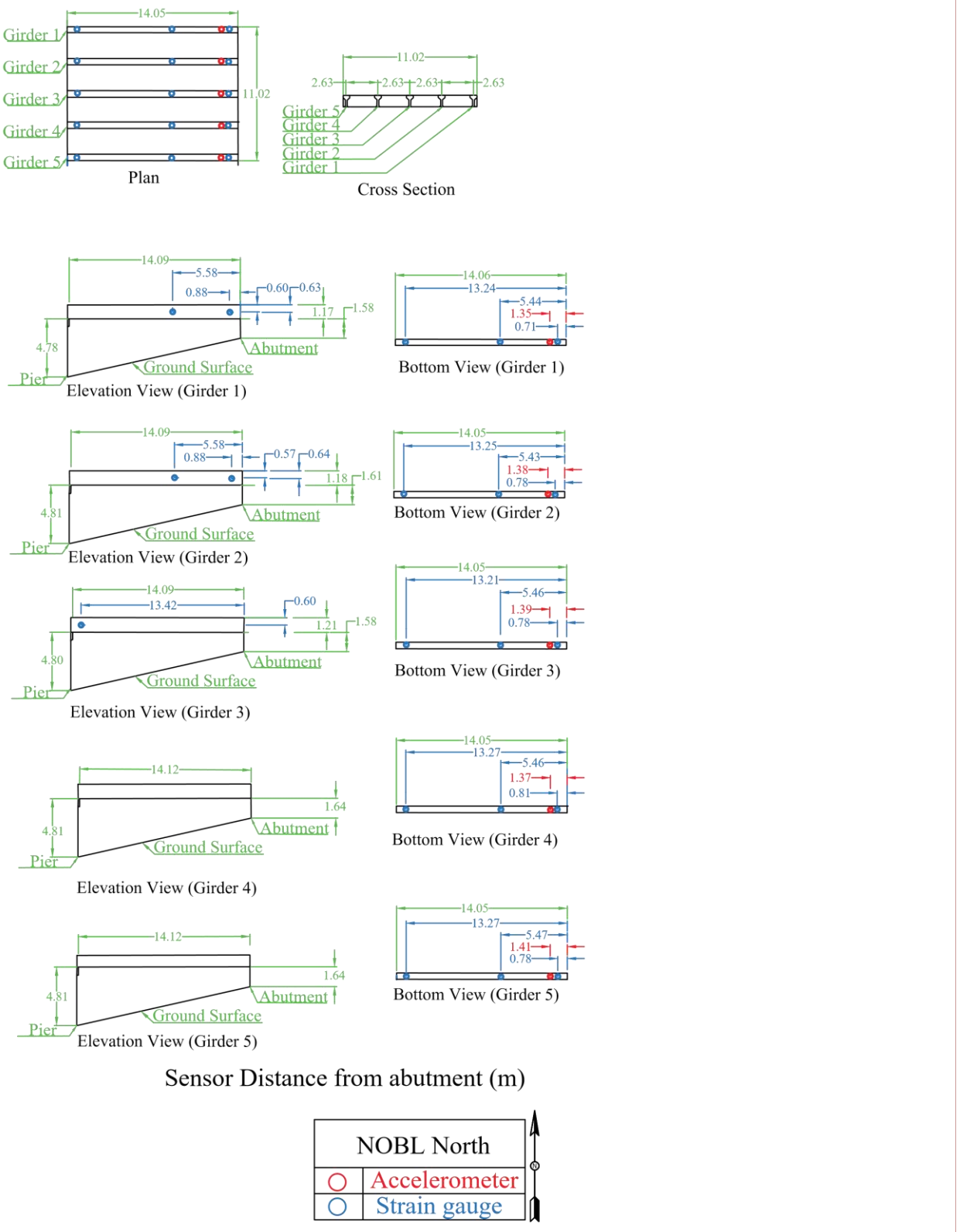

Figure 4.4. Locations of the accelerometers instrumented to girders for NOBL North.

4.5 Test procedure and truck arrangement

In this research and to quantify the bridge behavior under traffic loads, two triaxial trucks with known weights passed through the bridges many times with previously defined speed and spacings. Figure *4.5* shows the two trucks passing through the bridge. The test trucks were 3-axle vehicles with different weights, where one truck denoted as number one was 50,400 lb, and truck denoted as number two of 30,560 lb. Figure *4.6* shows the two trucks used for this bridge loading test at the NOBL West bridge at Yutan. The acceleration values were recorded for every single truck pass, as a function of time, and for both two trucks as side-by-side and back-to-back in one or two different traffic lanes. The tests were repeated for approximately sixty times for each of the bridges with various speeds ranging from 5-60 miles per hour. The load combination for NOBL North bridge is shown in Table 4.1. Load combinations related to the other two bridges can be found in appendix B, which closely mimics that of the NOBL North bridge.

(a) side-by-side truck passing

(b) Back-to-back truck passing

Figure 4.5. Example of side-by-side and back-to-back truck passing load test.

Table 4.1. Live load test for NOBL North bridge.

Run #	Dir.	Speed (mph)	Truck No.	Lane
1	W[1]	5	1	C [3]
2	E [2]	5	1	C
3	W	5	1	C
4	E	5	1	C
5	W	10	2	C
6	E	10	2	C
7	W	10	2	C
8	E	10	2	C
9	W	20	1	C
10	E	20	1	C
11	W	20	1	C
12	E	20	1	C
13	W	40	2	C
14	E	40	2	C
15	W	40	2	C
16	E	40	2	C
17	W	60	1	C
18	E	60	1	C
19	W	60	1	C
20	E	60	1	C
21	W	10	1	N [4]
22	E	10	1	N
23	W	10	1	S [5]
24	E	10	1	S
25	W	40	1	N
26	E	40	1	N
27	W	40	1	S
28	E	40	1	S
29	W	60	1	N
30	E	60	1	N
31	W	60	1	N
32	E	60	1	N
33	W	60	1	S
34	E	60	1	S
35	W-W [6]	10-10	2-1	S-N [8]
36	E-E [7]	10-10	2-1	S-N
37	W-W	10-10	2-1	S-N
38	E-E	10-10	2-1	S-N
39	W-W	40-40	2-1	S-N
40	E-E	40-40	2-1	S-N
41	W-W	60-60	2-1	S-N

42	E-E	60-60	2-1	S-N
43	W-W	60-60	2-1	S-N
44	E-E	60-60	2-1	S-N
45	W	5	1	N^{+} (9)
46	E	5	1	N^{+}
47	W	5	1	N^{+}
48	E	5	1	N^{+}
49	W/W (10)	10/10	1/2	N/N (12)
50	E/E (11)	10/10	1/2	N/N
51	W/W	10/10	1/2	S/S (13)
52	E/E	10/10	1/2	S/S
53	W/W	40/40	1/2	N/N
54	E/E	40/40	1/2	N/N
55	W/W	40/40	1/2	S/S
56	E/E	40/40	1/2	S/S
57	W/E	40/40	1/2	N/S (14)

1. Truck pass from East to West direction.
2. Truck pass from East to West direction.
3. Truck pass through the center of the bridge.
4. Truck pass through the North Lane of the bridge.
5. Truck pass through the South Lane of the bridge.
6. Trucks pass side-by-side from East to West direction.
7. Trucks pass side-by-side from West to East direction.
8. Trucks pass side-by-side in North and South Lane.
9. 2 [ft] away from the North edge of the North Lane.
10. Trucks pass back-to-back from East to West direction.
11. Trucks pass back-to-back from West to East direction.
12. Trucks pass back-to-back in the North Lane.
13. Trucks pass back-to-back in the South Lane.
14. Trucks pass back-to-back in the North and South Lane.

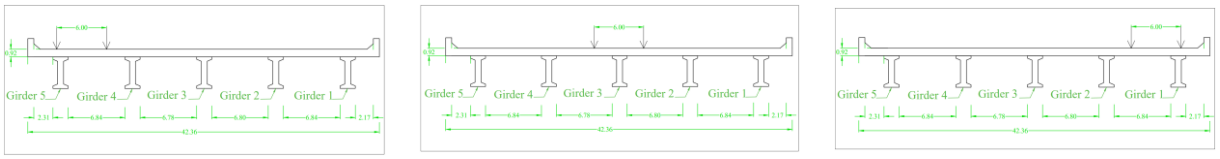

(a) North lane with 2 feet away from the curb (b) center lane (c) South lane with 2 feet away from the lane

Figure 4.6. Truck loading path at the NOBL North bridge at Omaha .

4.6 Analyzed data

The accelerometer data was processed in the time and frequency domain to apply instrument calibration factors and filtering. The data was processed using a Hampel filter for noise spikes and a finite impulse response (FIR) filter of order 4096 over two distinct ranges. The filtering range for the Yutan steel bridges was 2-25 Hz and for the Omaha concrete bridge at NOBL North from 5-25 Hz. This range varied slightly to capture only the lowest frequencies that correspond to the first mode. Using the processed data, frequencies can be determined as well as the maximum acceleration envelopes. The upcoming sections will provide a summary of each method.

4.6.1 Stochastic subspace identification

Stochastic subspace identification (SSI) is an algorithm that is commonly used to extract structural vibration characteristics from operational vibration measurements. Specifically in this project, the extended unweighted principal component method provided clear results (Martindale et al., 2019) using the Artemis platform (Döhler et al., 2017). Comparing these values for two of the bridge sites on ambient vibrations (not during the live loads), the first three modes of each bridge are experimentally (denoted as SSI) determined as summarized in Table 4.2. The results show very a good match with each other and consequently, the initial FEA models did not require an update for general usage. The first or primary mode of each structure was analytically captured within 3%, indicating an extremely good match. Note, that ambient vibrations were not collected at the NOBL East bridge at Yutan.

Table 4.2. Frequency of the bridge based on the stochastic subspace identification.

Mode	NOBL West Frequency (Hz)			NOBL North Frequency (Hz)		
	SSI	FEA	Percent difference	SSI	FEA	Percent difference
1	2.71	2.77	2.2	9.57	9.29	2.9
2	3.09	3.02	2.3	10.5	9.78	6.9

4.6.2 Maximum acceleration envelopes

The acceleration data can provide valuable information about the natural frequency, displacement, and dynamic characteristics of the bridge. Using the processed time histories, peak acceleration values can be determined for each test (or live load run) for a given location on the bridge. Figure *4.7* and Figure *4.8* shows the accelerometer peak values determined by each test (each truck run) at NOBL North. These plots indicate the peak values by each channel (each sensor) where the peak values obtained by the channel are shown in Figure *4.9*. Using these peak values, an envelope of the maximum acceleration experienced can be done for each live load run. This highlights the maximum response for a given location on the bridge and has been interpolated, not that the piers are presumed to have no acceleration. These acceleration maps identify the maximum acceleration envelopes and can be used to validate models and other future usages. Note that the figures presented here show the deck and girder time histories for NOBL North, where the complete set is in Appendix B.

4.7 Intermediate conclusions

Task 3 of this project provides an example facility demonstration. Under the guidance of the project team and the TAC panel, this resulted in an extensive live load test at each bridge. Within the live load tests, acceleration and strain datasets were captured and processed. This chapter outlined and summarized the acceleration data, including acceleration envelope data, which indicate the maximum acceleration for a given live load run. The next chapter will outline the strain data processing for NOBL North. The experimental datasets are available for use by request. It is also envisioned that this experimental data will support the project's goal of establishing a research and educational facility related to bridge health and the training of students/future engineers, bridge engineers, and bridge inspectors.

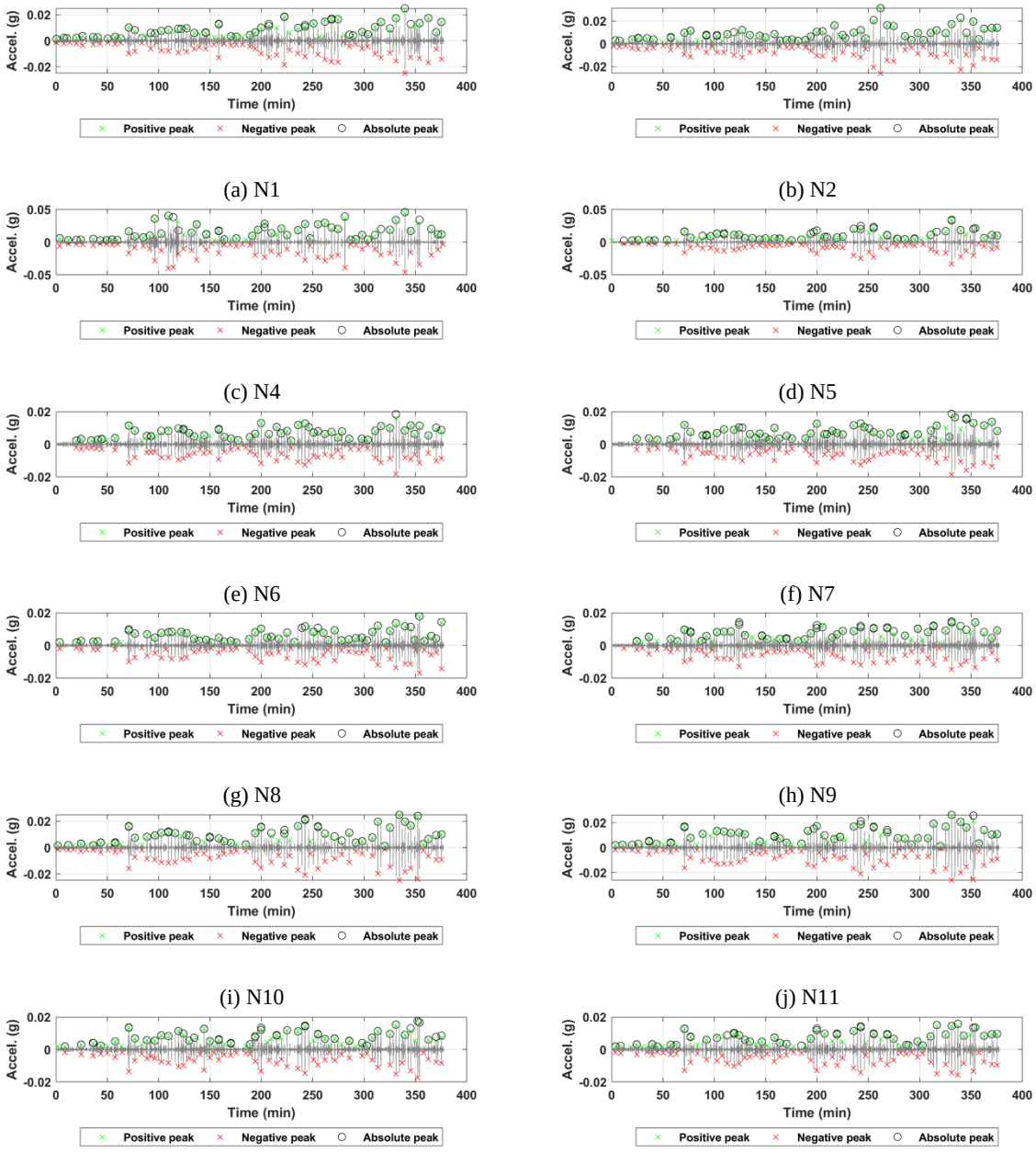

(a) N1 (b) N2

(c) N4 (d) N5

(e) N6 (f) N7

(g) N8 (h) N9

(i) N10 (j) N11

(k) N12 (l) N13

Figure 4.7. Acceleration time histories of the deck sensors for all truck passes at NOBL North.

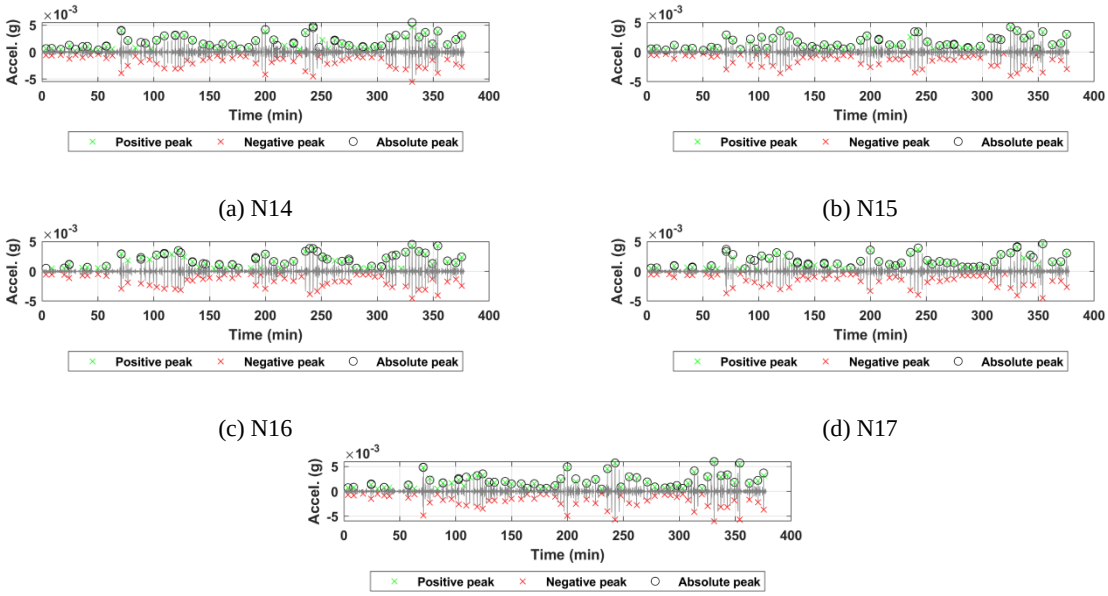

(a) N14

(b) N15

(c) N16

(d) N17

(e) N18

Figure 4.8. Acceleration time histories of the girder sensors for all truck passes at NOBL North.

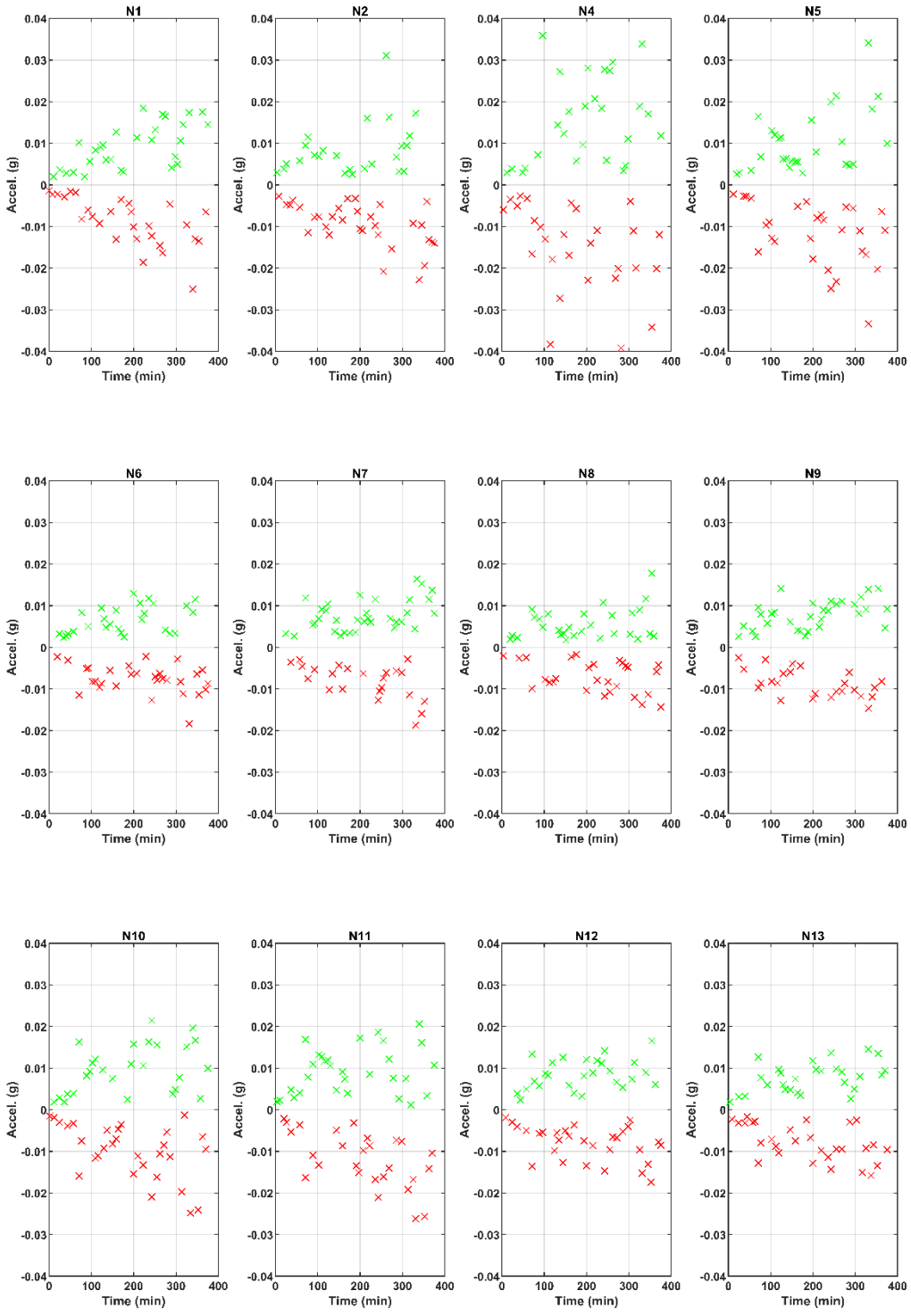

Figure 4.9. Maximum acceleration values for each truck pass at the NOBL North.

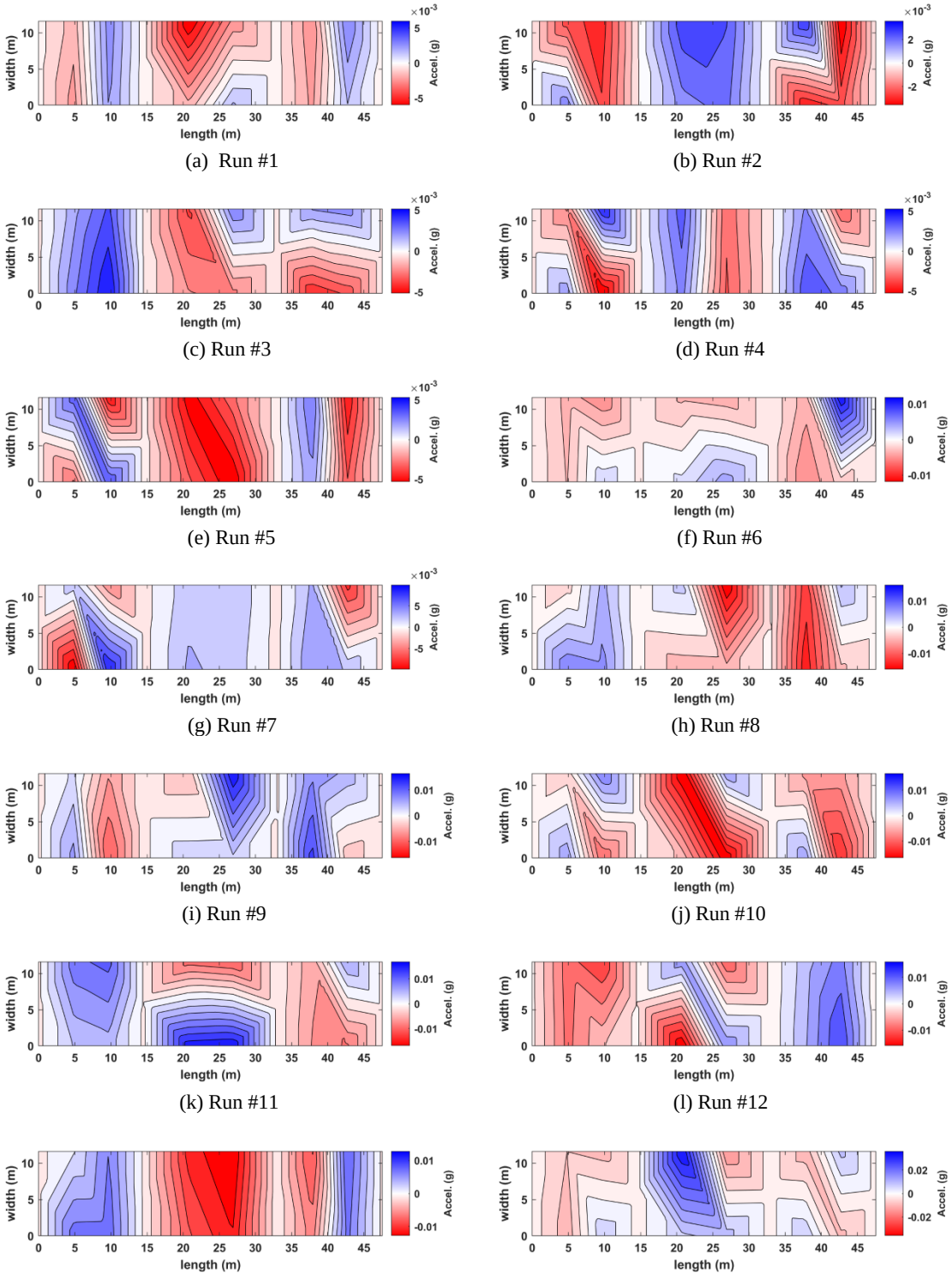

(a) Run #1 (b) Run #2

(c) Run #3 (d) Run #4

(e) Run #5 (f) Run #6

(g) Run #7 (h) Run #8

(i) Run #9 (j) Run #10

(k) Run #11 (l) Run #12

(m) Run # 13 (n) Run #14

Figure 4.10. Interpolated acceleration in plan view for 14 trucks passing at the NOBL North. Note the bridge is oriented to the north direction (up on the page is north).

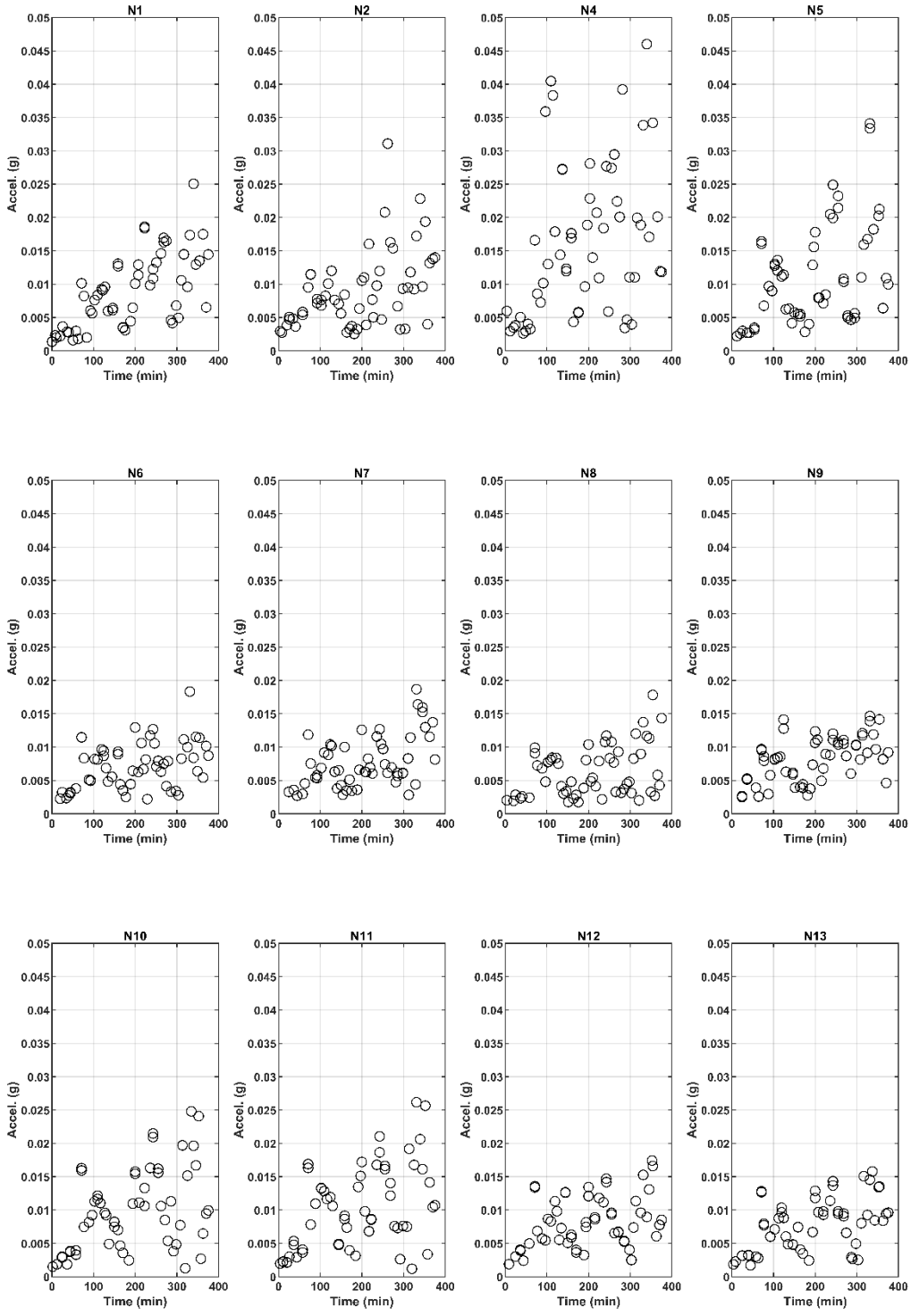

Figure 4.11. Absolute maximum acceleration values for each truck pass at the NOBL North.

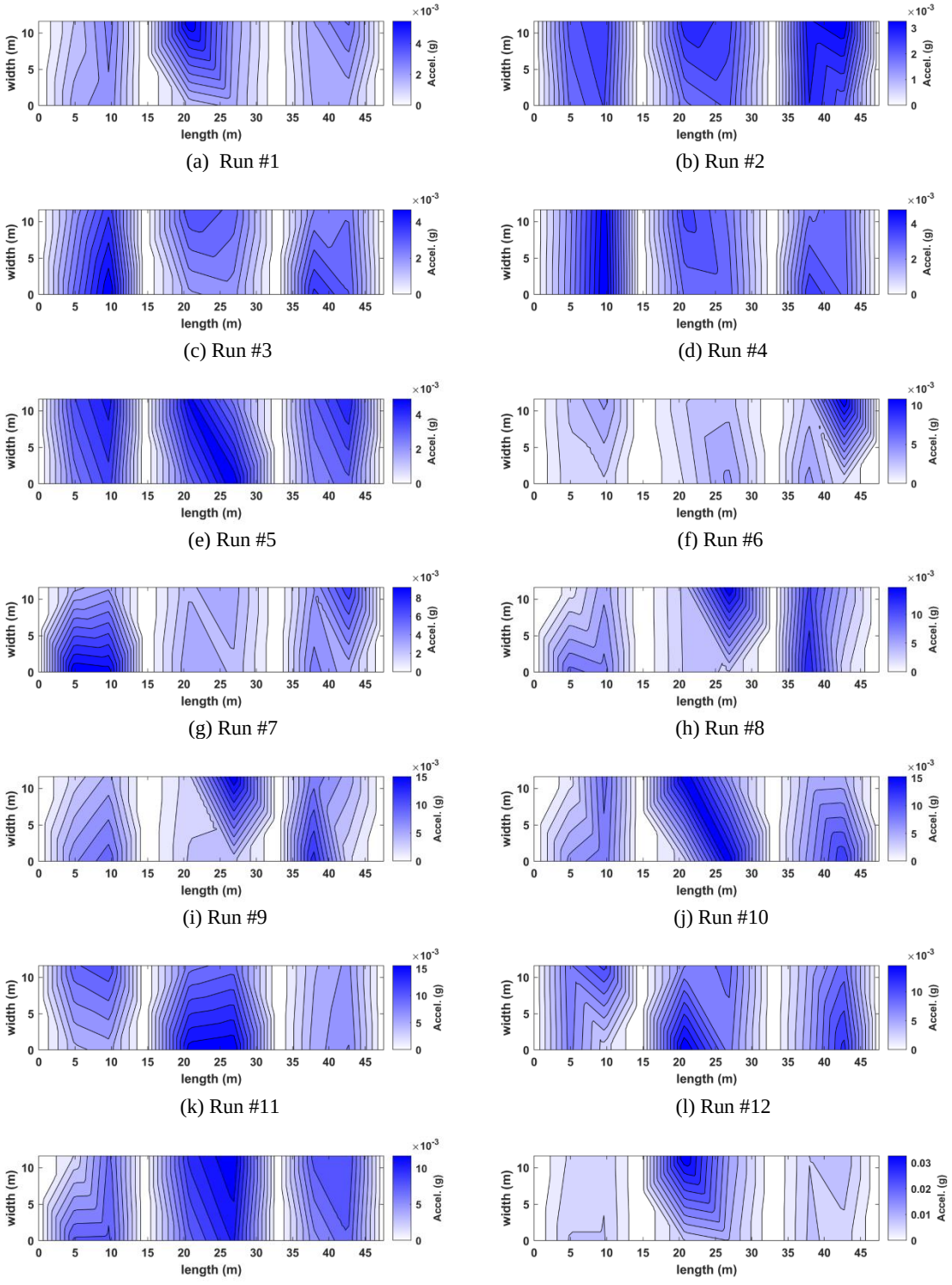

(a) Run #1 (b) Run #2

(c) Run #3 (d) Run #4

(e) Run #5 (f) Run #6

(g) Run #7 (h) Run #8

(i) Run #9 (j) Run #10

(k) Run #11 (l) Run #12

(m) Run # 13 (n) Run #14

Figure 4.12. Interpolated absolute-valued acceleration in plan view for 14 truck passings at the NOBL North. Note the bridge is oriented to the north direction (up on the page is north).

5 Strain gauge and updated FE models

5.1 Overview

This chapter provides a brief overview of load testing and analytical modeling performed for NOBL North at Omaha with a particular focus on strain gauges. Refer to Appendix C for additional data and discussion related to testing and modeling for this bridge supplementary to the information provided in this chapter. This chapter is included as a stand-alone given its detailed focus on the NOBL North site.

Strains measured during field tests were compared with analytical calculations. Finite element models (FEMs) in 2D and 3D were developed for this bridge using SAP2000, CSiBridg, AASHTOWare BrR, and COMSOL. Construction plans, initial site characterization geometric data, and supplementary correspondence provided by the Nebraska Department of Transportation (NDOT) primarily guided the geometry and material properties implemented in the bridge models. The analytical studies included explorations of various modeling assumptions, such as rotational restraint applied to the girder superstructure by abutments and piers.

Girder distribution factors (GDFs) quantify the proportion of live load carried by individual girders and are a common focus of field testing evaluations. The load test results were compared to AASHTO LRFD (2020) and AASHTO Standard Specifications (2002) approximate GDFs, and to GDFs determined from 3D FEMs. This study included an investigation of actual dynamic load amplification factors by comparing bridge responses when subjected to trucks traveling at varying speeds.

5.2 Prestressed Concrete Bridge Details

NOBL North at Omaha has nominal span lengths of 48, 60, and 48 ft, as shown in Figure 5.1. The bridge is comprised of five Nebraska Type 3A girders spaced at 8 ft 8 in, as shown in Figure 5.2 with 0-degree skew. The average deck thickness is 7.5 in., and the overhang is 3 ft-10 in. Refer to Chapter 2 for additional details.

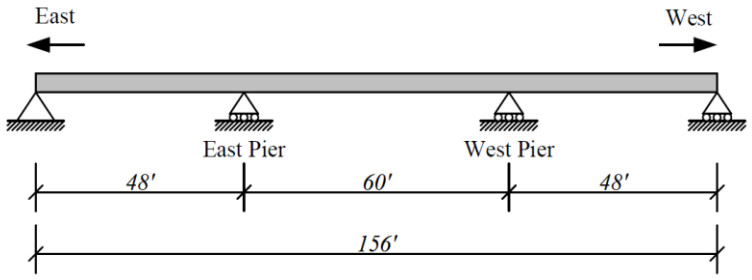

Figure 5.1. Schematic elevation of the bridge.

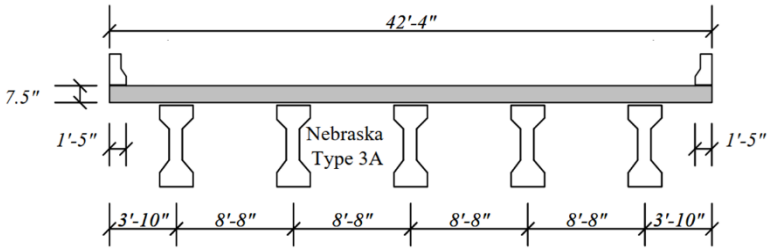

Figure 5.2. Schematic cross-section of the bridge.

5.3 Instrumentation

ST350 strain transducers from Bridge Diagnostics Inc (BDI) were installed on four cross-sections of the bridge, as shown in Figure 5.3. ST350 data was sampled at sufficiently high strain rates to capture dynamic strain amplification. Tests described herein were the short term and strain readings were zeroed at the start of each test run so that any thermally-induced strains were neglected.

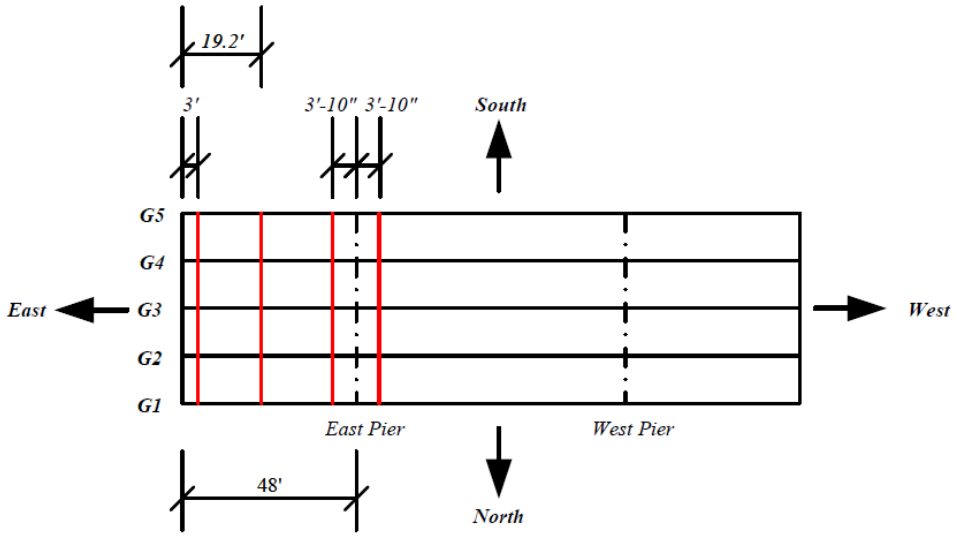

Figure 5.3. Strain transducers installation locations in the bridge.

The strain transducers were positioned 3 ft from the east abutment bearings' centerline. Similarly, maximum negative bending moments of the simple-made-continuous bridge were anticipated and investigated near the piers by installing strain transducers 3 ft away from the bearing centerlines on the east and west sides of the east pier. Each bearing centerline was offset 10 inches from the pier centerline, so that strain gages were located 3 ft-10 in. from the pier centerline. The positive moment was monitored at 0.4L of the east end span (19.2 ft to the east abutment centerline).

A total of forty-four (44) strain transducers were attached at the four selected cross-sections. Figure 5.4 shows the strain locations on the girder and the bottom of the concrete deck. On each girder, strain transducers were attached to the center of the bottom flange. Additionally, girder web strain transducers were installed to determine the neutral axis and evaluate the bridge behavior of non-composite and composite sections. A strain transducer was attached to the bottom of the concrete deck 2 in. from the side of the top flange of the center girder (G3) for each cross section. Transducers were attached to the concrete with adhesively bonded metal tabs, as shown in Figure 5.5.

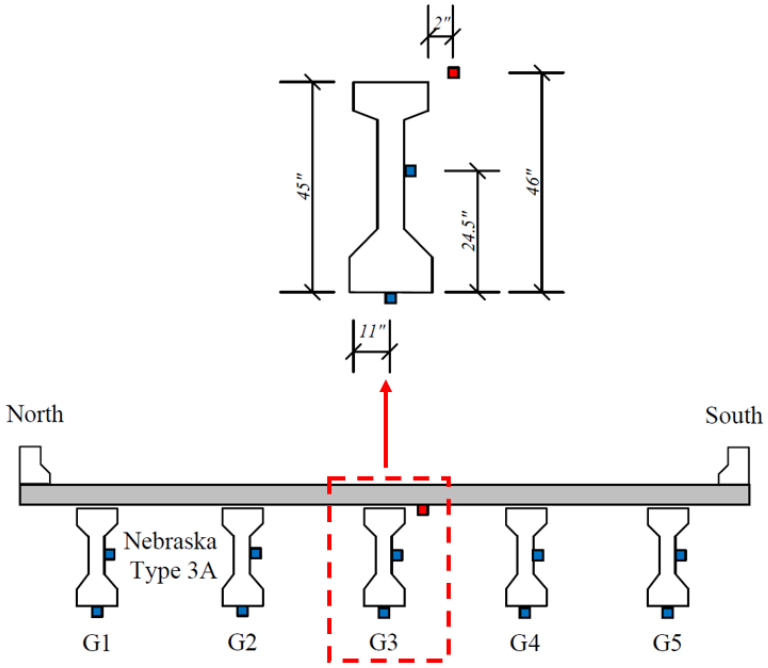

Figure 5.4. Strain transducers installation locations in the bridge cross-section.

Figure 5.5. Strain transducer attached to the bottom flange of girder.

5.4 Load Cases

Two 3-axle trucks (Legal Type 3 vehicles) were provided by NDOT for NOBL North loading. Figure 5.6 shows one of the trucks used in the load tests. Only total truck weight was supplied, not weight by axle or wheel, so each test truck axle load was assumed to be proportional to the Nebraska Legal Type 3 configuration. Girder distribution factors were evaluated by driving trucks across the bridge at various transverse locations, as illustrated in Figure 5.7. A total of 32 load tests were performed, with various combinations of one or both trucks, truck directions, truck transverse positions, and speeds from crawling (approximately 5 mph) up to about 60 mph. Refer to Appendix C for additional details.

Figure 5.6. Load test truck A.

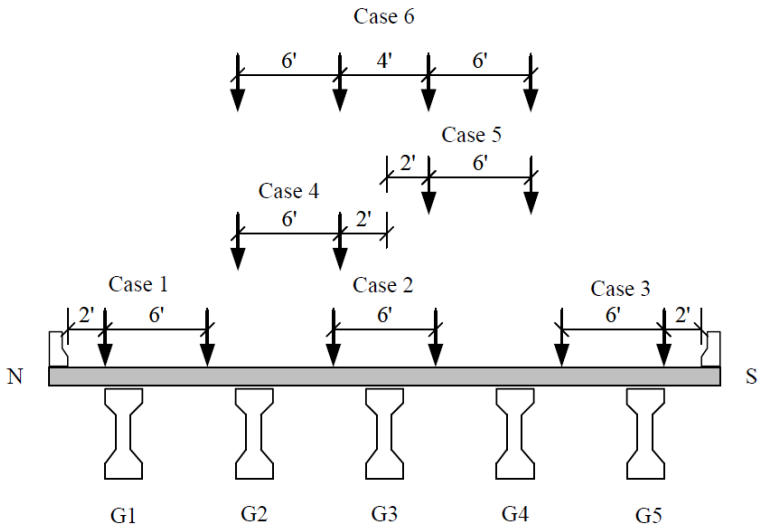

Figure 5.7. Transverse locations of trucks on the bridge.

5.5 Finite Element Analysis (FEA)

For this study, both two-dimensional (2D) and three-dimensional (3D) finite element analyses (FEA) were applied to investigate structural behavior. Analyses were performed using SAP2000™, CSiBridge™, AASHTOWare Bridge Rating™ (BrR), and COMSOL™ finite element programs. The following types of models were used:

Line-girder analysis:

- SAP2000 model with beam elements,

3D FEM analysis:

- 3D CSiBridge model with shell elements for slab and beam elements for girders,
- 3D AASHTOWare BrR model with shell elements for slab and beam elements for girders,
- 3D COMSOL model with solid elements for slab and girders.

Refer to Appendix C for additional details.

5.6 Load Test and FEM Results

CSiBridge results were used for comparison to the test results. To compare the test results with FEA models, the FEA values were taken at the locations where strain transducers were installed.

5.6.1 Load Test Strain Plotted with Time

Transducers located at 0.4L of the east end span measured the positive moment response and were used to quantify GDFs. As truck A crawls at approximately 5 mph from east to west at the center, Figure 5.8 shows the measured values for the transducers at 0.4L of the end span. Time (seconds) is shown on the x-axis, and microstrain ($\mu\varepsilon$) is shown on the y-axis. As expected for Run 1, peak strains occurred on the bridge's middle girder (G3). At the bottom of G3, the maximum strain value is about +32 $\mu\varepsilon$. Because of the intended

transverse symmetrical load position, the strains for G2 and G4 should be similar. However, G4 has greater strains than G2 presumably due to a slightly off-center transverse truck positioning.

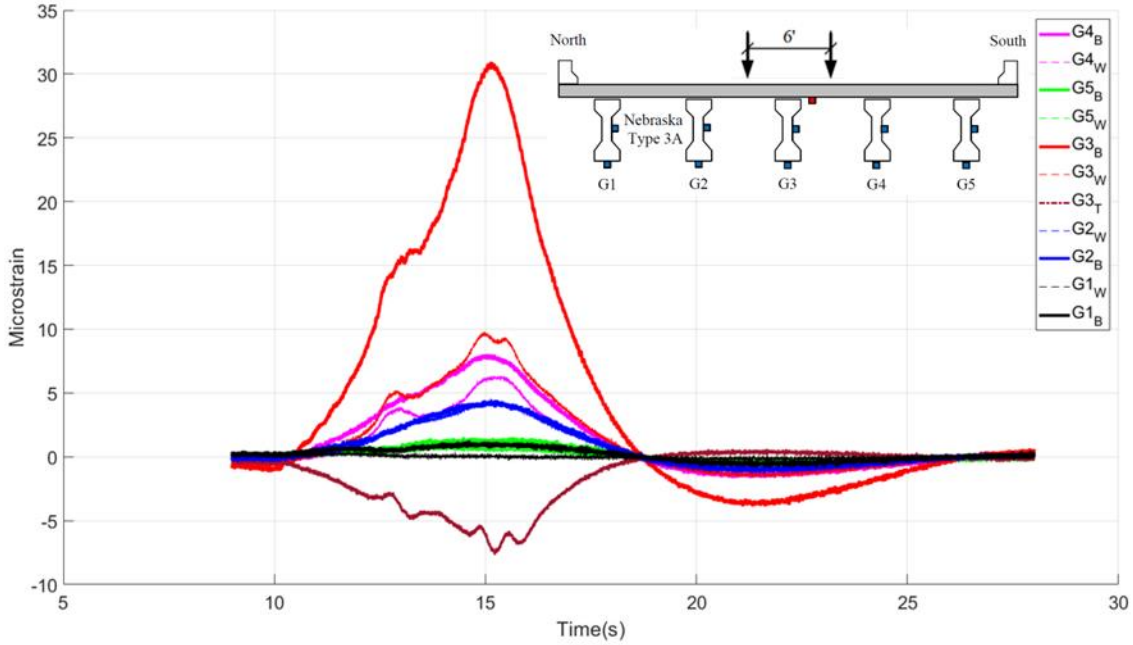

Figure 5.8. Strain transducer results at 0.4L end span for one truck A at the center from east to west.

Unexpectedly, the test strains at G2 are similar at the bottom flange and the web, implying axial rather than flexural deformation. This result does not seem reasonable, yet the recorded strains are nonzero and outside the noise band, suggesting that the data is real and not spurious noise. This abnormality may reflect torsional influences on the girder cross-section strains that could have obfuscated the primary flexural response. In situations where loads travel along the center of the bridge width, exterior girders G1 and G5, as expected, carried a lesser load. Refer to Appendix C for additional details.

5.6.2 Test and FEM Strain and GDF Results

GDFs were determined using strain data measured at the bottom of the girders. This project used the same GDF model as Stallings and Yoo (1993). The Wi was assumed to be one for both interior and exterior girders, which slightly overestimated interior girder GDFs and underestimated exterior girder GDFs. To

make comparisons with AASHTO LRFD GDFs, the GDF model has been modified to account for the number of lanes loaded.

The following load test GDFs are based on single or two trucks traveling at low speeds for various transverse locations. FEM GDFs were derived from CSiBridge models both with and without diaphragms. Figure 5.9 and Figure 5.10 show the bottom girder strains at 0.4L of the end span and corresponding GDFs for one truck traveling from east to west along the bridge centerline and 2 ft from the north and south barrier railings. Figure 5.9 shows that, as expected, the maximum strain occurred at G3 for center lane cases and exterior girders (G1 or G5) for trucks passing adjacent to barriers. However, there are some noticeable differences between strains from load tests and FEMs. With single-lane loading at the center, the maximum positive strain at G3 is about +31 με, close to the FEM at G3 for the model without diaphragms. However, other girders exhibit lower load test strain results than FEM. The bottom flange load test strain sum in Figure 5.9 is about half that of FEM.

Possible reasons for the lower strains observed in load tests than in FEMs include partial fixity conditions at supports (although test data did not indicate this effect to be significant for this bridge), higher concrete moduli of elasticity than expected according to AASHTO, and potential stiffening from barriers. Figure 5.10 shows that the load test GDFs at 0.4L of the end span were more similar to the results of the FEM without diaphragms, which indicates that the diaphragms are not acting with transverse flexural continuity through the girders. On close inspection of the NOBL North bridge at Omaha drawings, the diaphragms are found to only interact with the girders through compression bearing. Reinforcing at the top of the diaphragms ties the diaphragms to the deck, but no reinforcing crosses the interfaces of diaphragms and girder flanges or webs. Therefore, complex torsional effects and compression-only contact interactions may also be influencing both flange and web strains that are currently unaccounted for in the 3D FEM models.

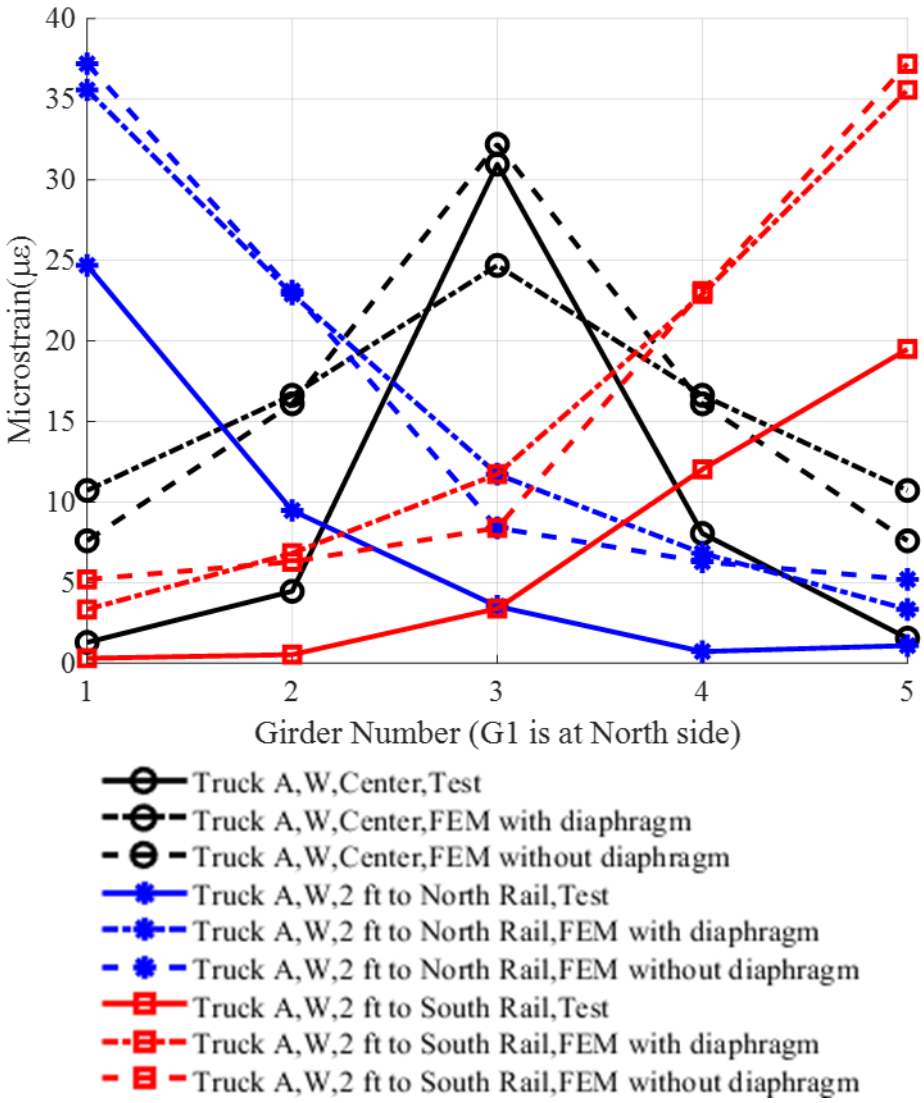

Figure 5.9. Positive strain at 0.4 L of east end Span, west direction loading.

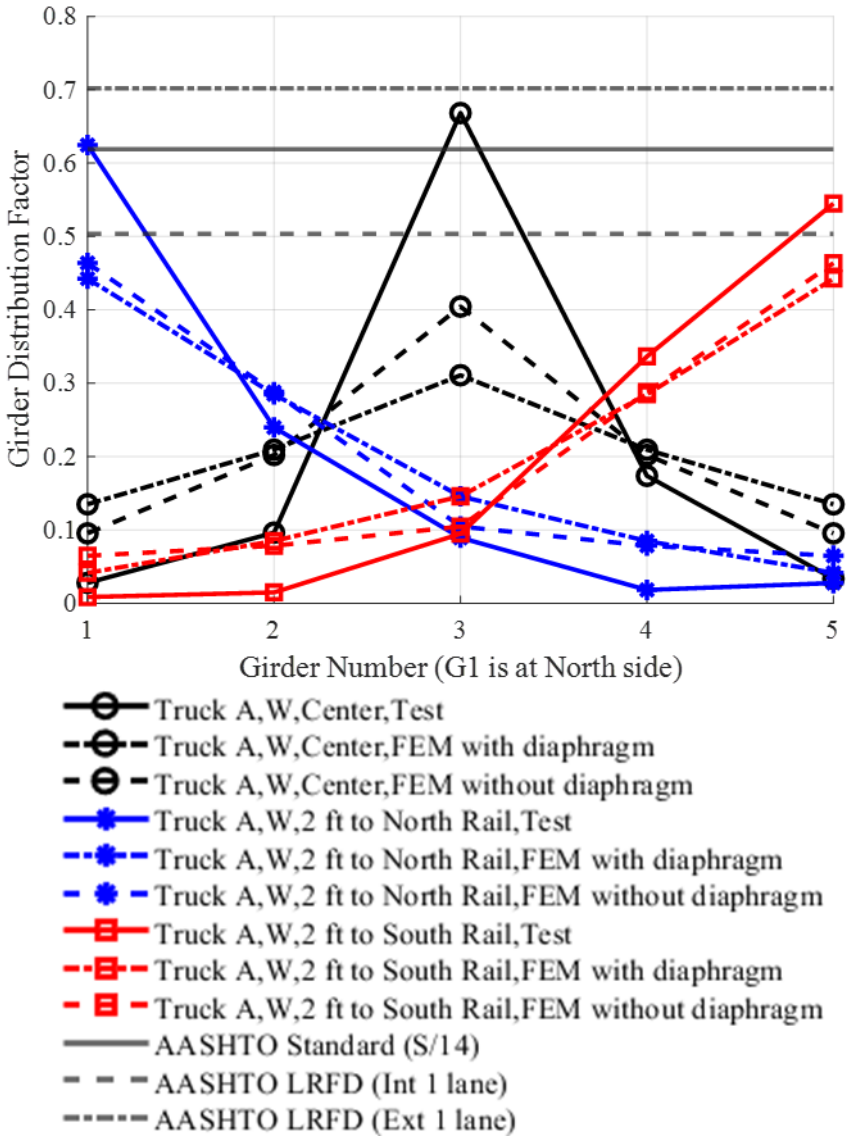

Figure 5.10. GDF from positive strain at 0.4 L of east end span, west direction loading.

5.6.3 Dynamic Load Allowance Results

Dynamic load factors (DLFs) were calculated as the ratio between the maximum dynamic strain and the maximum crawling speed (static) strain at the bottom of girders. DLFs were found to be negligible.

5.6.4 Neutral Axis Location

The neutral axis location was determined using an assumed linear strain profile through the depth of girders and pairs of strain measurements taken at the bottom flange and web. For Girder G3 at 0.4L along the end span, the neutral axis obtained from strain measurements was 36.22 in., only 3% lower than a theoretical composite section location of 37.39 in. obtained using as-built drawings for geometry and moduli of elasticity estimated according to AASHTO.

5.7 Intermediate conclusions

This stain gage task aimed to develop computational models representing the NOBL North bridge at Omaha (S036 02040L) and collect physical data to validate the FEM models. The models and load test data can be used by other researchers using the NOBL North site. During the field load tests, one-lane and two-lane loaded cases were taken into account to calculate the GDFs and DLFs and provide insight into the bridge behavior. NE Legal Type 3 trucks were used for the tests, and different locations, crawling speeds, and normal truck speeds were considered.

CSiBrdge, SAP2000, COMSOL, and AASHTOWare BrR were used to develop 2D line girder analysis and 3D FEMs. Shell, beam, and solid elements were used in the FEMs. CSiBridge models without barriers and with or without diaphragms were compared with load test results to determine if the model represents actual bridge behavior. Load tests and FEM analyses were also used to compare GDFs with AASHTO Standard (2002) and AASHTO LRFD (2020). Below are several takeaways from this chapter:

- The measured GDFs are generally close to those obtained from FEM analysis, but with some exceptions: For one truck or two trucks side-by-side in the center lane, GDF at G3 is higher than AASHTO interior GDFs (accounting for the Multiple Presence Factor (MPF)).
- Load test GDFs for exterior girders are smaller than AASHTO lever rule GDFs.
- For 0.4L of the end span, load test GDFs are more similar to computational results without diaphragms assumed continuous through girders.

- The sum of bottom girder load test strains is about half of the sum from FEM (potentially influenced by barrier participation, underestimated modulus of elasticity, partial fixity of supports in the natural bridge, and perturbation of measured strains by torsional effects).
- Load tests observed localized behavior near piers at the bottom of the concrete deck inconsistent with beam theory, likely a result of concentrated wheel loads near instrument locations.

The results indicate that the trends of strains and GDFs between load tests and FEMs are reasonably close; however, the magnitudes have some noticeable differences. The load tests recorded lower strains than predicted by the FEMs, possibly because some structural parameters (barriers at the middle span, diaphragms, modulus of elasticity, etc.) were not measured, complex torsional stress and strain fields perturbed the measurements, or due to hardware, software, or user errors with the strain transducer system. Future research would be beneficial to instrument diaphragms and barriers in positive moment regions to improve understanding of diaphragm behavior, update load distributions, estimate composite barrier participation, and more closely examine potential torsional effects in girders. Strain transducers could also be installed on one or both piers to investigate vertical strains associated with continuity participation and braking loads. It is also recommended that the load test be performed with heavier loads and that the modulus of elasticity be verified with non-destructive testing.

6 Future work and summary

6.1.1 Overview

The goal of this unique project was to establish the Nebraska Outdoor Bridge Lab (NOBL). The NOBL facility is located at two sites, Yutan and Omaha, Nebraska. It consists of three bridges, two steel bridges over the Platte River at Yutan as well as one concrete bridge over the Glenn Cunningham Reservoir at Omaha. All of these bridge sites are minimally not in regular service or completely out of service. The NOBL facility aims to become a national research and educational facility for bridge health and testing. This means supporting various stakeholders, including the University of Nebraska-Lincoln (UNL), other academic or research entities, the Nebraska Department of Transportation (NDOT), other transportation departments, practicing engineers, equipment/technology vendors, and the greater community. This facility aims to provide unique opportunities for students/future engineers, bridge engineers, bridge inspectors, and any other interested parties.

- To establish this facility, four tasks were completed and summarized in this document. Tasks included (1) Site Staging, (2) Site Characterization, (3) Facility Demonstration, and (4) Reporting. Within this project, the following key accomplishments were made:
- A safety and operational document summarize activities, procedures, and risks at this laboratory facility. This document is available on the NOBL project's website.
- The two steel bridge structures at Yutan were secured via fencing to create a safe laboratory environment.
- High-fidelity and high-detailed geometric surveys were conducted of all the bridge sites using lidar and uncrewed aerial systems. This provides accurate data at the centimeter level on the current condition of these structures. This data can be viewed on the NOBL project's website.
- Finite element analysis (FEA) models were constructed for all the bridge sites within the CSiBridge software platform.

- Ground penetrating radar surveys were conducted on all the bridge sites to quantify the condition of the bridge decks as well as the approach slabs.
- An extensive field demonstration was done at all three bridge sites. This involved an array of sensors to quantify the dynamic bridge behavior under various truckload combinations. Live loads included two 50-kip (nominal) weight triaxial trucks that loaded the bridges at various speeds, patterns, spacings, etc. Each bridge was subjected to approximately 60 different loading configurations. This data has been processed, filtered, compiled, and available for use by others upon request.
- A detailed strain gauge study was conducted at NOBL North and summarized as part of the site demonstration.
- The site demonstration was conducted in collaboration with external researchers from SC Solutions and its subaward grants to the University of Nevada-Reno and the University of California, Los Angeles. Ongoing collaborative work continues in publishing and marketing this data which will also increase the visibility of the site.

6.1.2 Online presence and available data

A critical part of this project is marketing and establishing a baseline set of data for use by others. To this end, the NOBL project has a dedicated website at http://nobl.unl.edu. This webpage exists at the University of Nebraska-Lincoln College of Engineering level for an extended lifespan. This website provides an overview of the project, the site, and describes some of the data available. This site will also host the final report for this project as well. Moreover, the generated datasets from this project are available for use by others by request. The available data includes for all bridge sites:

- Plan drawings.
- High-fidelity and high-detailed geospatial datasets in terms of three-dimensional point clouds and 2D orthomosaic images.

- Constructed finite element analysis (FEA) models in CSiBridge.
- Constructed FEA models in other platforms for the NOBL North bridge site only. This includes SAP2000, CSiBridg, AASHTOWare BrR, and COMSOL.
- Ground penetrating radar survey data and (likely) delamination maps.
- Extensive accelerometer and strain gage data from the experimental campaign (as detailed in Chapters 4 and 5)

For interested parties concerning NOBL site usage or data availability/sharing, please use one of the following methods:

- Online form submission (google forms) at: **https://forms.gle/4SgMcpUoPCQgMyCt7/**
- Email the site principal investigator, Prof. Richard L. Wood at: **rwood@unl.edu**
- If the above two methods do not provide a response within a week or so, please call or send an email inquiry to the UNL Department of Civil and Environmental Engineering

6.1.3 Future site usage plans

Since the establishment of this site, the site has been used by non-UNL personnel including NDOT, NSP, Omaha Police Department, and the Nebraska Wing of Civil Air Patrol (Fremont Cadet Squadron) . Some of the current plans for the use of this site include current and pending research projects at UNL as well as potentially at least six courses:

- CIVE 102 – Introduction to Geomatics for Civil Engineers
- CIVE 441 – Steel Design I
- CIVE 443/843 – Advanced Structural Analysis
- CIVE 839 – Bridge Design
- CIVE 891 – Non-Destructive Testing Methods

- CIVE 891 – Infrastructure Assessment Techniques

6.1.4 Future research needs

As this project progressed and with conversations with internal and external stakeholders, some future research needs include:

- Coring of the deck at select locations to confirm deck delamination.
- Live load testing with large loads to confirm/verify the elastic modulus of various bridge elements.
- Verification of load redistribution by undoing various assemblies (inclusive of the pin and hanger connections at Yutan).
- Controlled scour simulations and the effect on the superstructures.
- Extreme loads (destructive in nature) that apply high temperature or river collision loads.
- Validation of various non-destructive/remote sensing technologies and methodologies.

7 References

1. American Association of State Highway and Transportation Officials (AASHTO). (2020). AASHTO LRFD Bridge Design Specifications, 9th Ed., Washington, DC.

2. American Association of State Highway and Transportation Officials (AASHTO). (2002) Standard Specification for Highway Bridges, 17th Ed, Washington, D.C.

3. Bose, S., Nozari, A., Mohammadi, M. E., Stavridis, A., Babak, M., Wood, R., ... & Barbosa, A. (2016). Structural assessment of a school building in Sankhu, Nepal damaged due to torsional response during the 2015 Gorkha earthquake. In Dynamics of Civil Structures, Volume 2 (pp. 31-41). Springer, Cham.

4. Döhler, M., Andersen, P., & Mevel, L. (2017, May). Variance computation of modal parameter estimates from UPC subspace identification. In *IOMAC-7th International Operational Modal Analysis Conference*.

5. Liao, Y., Mohammadi, M. E., Wood, R. L., & Kim, Y. R. (2020). *Improvement of Low Traffic Volume Gravel Roads in Nebraska* (No. SPR-P1 (16) M040).

6. Martindale, G., Watson, D., Kodsy, A. M. K., El-Khier, M. A., Wood, R. L., & Morcous, G. (2019). *Performance evaluation of inverted tee (IT) bridge system* (No. Report No. 2611214037-001). Nebraska. Department of Transportation.

7. NOBL. (n.d.). Retrieved from https://engineering.unl.edu/outdoorbridgelab/

8. Ocel, J. M. (2021). *Historical Changes to Steel Bridge Design, Composition, and Properties* (No. FHWA-HRT-21-020). United States. Federal Highway Administration. Office of Infrastructure Research and Development.

9. Pashoutani, S., & Zhu, J. (2020). Ground penetrating radar data processing for concrete bridge deck evaluation. J. Bridg. Eng, 25, 04020030.

10. SC Solutions. (n.d.). Retrieved from https://www.scsolutions.com/sc-solutions-awarded-phase-ii-of-the-small-business-innovative-research-sbir-program-to-develop-digital-twin-and-computer-vision-technology-for-operational-monitoring-and-maintenance-of-bridges/

11. Stallings, J. M., & Yoo, C. H. (1993). Tests and ratings of short-span steel bridges. *Journal of Structural Engineering*, 119(7), 2150-2168. https://doi.org/10.1061/(ASCE)0733-9445(1993)119:7(2150).